

1-1-2007

Effect of photovoltaic (PV) module mounting angle on PV module power output

Husam Hamdi Alkhatib
Ryerson University

Follow this and additional works at: <http://digitalcommons.ryerson.ca/dissertations>

 Part of the [Electrical and Computer Engineering Commons](#)

Recommended Citation

Alkhatib, Husam Hamdi, "Effect of photovoltaic (PV) module mounting angle on PV module power output" (2007). *Theses and dissertations*. Paper 230.

This Thesis Project is brought to you for free and open access by Digital Commons @ Ryerson. It has been accepted for inclusion in Theses and dissertations by an authorized administrator of Digital Commons @ Ryerson. For more information, please contact bcameron@ryerson.ca.

EFFECT OF PHOTOVOLTAIC (PV) MODULE MOUNTING ANGLE ON PV MODULE POWER OUTPUT

By

Husam Hamdi Alkhatib

A Final Project Report

presented to Ryerson University

in partial fulfillment of the

requirements for the degree of

Master of Engineering

in the program of

Electrical and Computer Engineering

Toronto, Ontario, Canada 2007

© Husam H Alkhatib 2007

UMI Number: EC53635

INFORMATION TO USERS

The quality of this reproduction is dependent upon the quality of the copy submitted. Broken or indistinct print, colored or poor quality illustrations and photographs, print bleed-through, substandard margins, and improper alignment can adversely affect reproduction.

In the unlikely event that the author did not send a complete manuscript and there are missing pages, these will be noted. Also, if unauthorized copyright material had to be removed, a note will indicate the deletion.



UMI Microform EC53635
Copyright 2009 by ProQuest LLC
All rights reserved. This microform edition is protected against
unauthorized copying under Title 17, United States Code.

ProQuest LLC
789 East Eisenhower Parkway
P.O. Box 1346
Ann Arbor, MI 48106-1346

Author's Declaration

I hereby declare that I am the sole author of this report

I authorize Ryerson University to lend this report to other institution or individuals for the purpose of scholarly research.

Date

Signature

Husam Alkhatib

I further authorize Ryerson University to reproduce this report by photocopying or by other means, in total or in part, at the request of other institutions or individuals for the purpose of scholarly research.

Date

Signature

Husam Alkhatib

Abstract

Solar energy is a renewable resource that is environmentally friendly. Unlike fossil fuels, solar energy is available just about everywhere on earth. This source of energy is free, immune to rising energy prices. Solar energy can be used in many ways - to provide electricity, heat, lighting, and mechanical power. The objective of this project is to determine the effect of mounting orientation of a photovoltaic panel on power output. Based on the simulation results, the report proposes alternative energy management techniques to characterize the unstable nature of the photovoltaic power generating system. A typical power generating system using photovoltaic technology would have many components.

The software used for determining the effects of photovoltaic module mounting angle on the PV module power output is the PV-DesignPro. This software is designed to simulate photovoltaic energy system operation on an hourly basis for one year, based on a user selected climate and system design.

Acknowledgments

I would like to take this opportunity to express my appreciation to Prof. R. Cheung for his teaching, guidance and great patience throughout the courses and project period. Without the teaching, supervision, suggestions and help of Prof. R. Cheung, it would have been impossible for me to complete this project.

Table of Contents

Declaration.....	ii
Abstract.....	iii
Acknowledgments.....	iv
Table of Contents.....	v
List of Tables.....	vi
List of Figures.....	vii
Chapter 1.....	1
Introduction.....	1
1.1 Objectives and Motivation.....	1
1.2 Background.....	2
1.3 General Approach to the Problem.....	3
Chapter 2.....	6
Literature Review.....	6
2.0 The Array as a System.....	6
2.1 Current-Voltage Characteristics.....	7
2.2 Reversible Effects of Temperature.....	9
Chapter 3.....	11
Statement of Problem and Methodology of Solution.....	11
3.1 Statement of Problem.....	11
3.2 Solution Methodology.....	11
Chapter 4.....	14
Simulation of PV Module Mounting Angle.....	14
4.1 PV module performance model used in the simulator.....	14
4.2 Effect of Irradiance on PV Module Performance Model.....	18
4.3 Photovoltaic (PV) Simulator.....	21
4.4 Simulation Results for the City of Toronto.....	23
4.5 Discussion.....	27
4.6 Energy Management.....	32
Chapter 5.....	36
Conclusion.....	36
5.1 Recommendations.....	37
Appendix A.....	39
Appendix B.....	40
Bibliography.....	42
Glossary.....	44
Index.....	45

List of Tables

Simulation results for module slope at 0 deg.....	24
Simulation results for module slope at 30 deg.....	25
Simulation results for module slope at 60 deg.....	26
Simulation results for module slope at 90 deg.....	27
0 deg vs 30 comparisons.....	28
90 deg vs 30 comparisons.....	29
90 deg vs 60 comparisons.....	30
60 deg vs 30 comparisons.....	31

List of Figures

Fig 2.0.1 The subsystem of an array.....	7
Fig 2.1.1a Solar cell electrical output characteristics; I.-V Curve.....	8
Fig2.1.1b Solar cell electrical output characteristics; P-V Curve.....	8
Fig2.2.1 Typical variations of solar cell current- voltage characteristics with temperature before (solid lines) and after (dashed lines) irradiation.....	10
Figure 3.2.1 Solution Methodology Flowchart.....	13
Figure 4.1.1 I-V curve reconstructed using the module performance model used in the simulator.....	17
Fig 4.2.1 Predicted effect of E_e on PV module voltage based on performance model.....	19
Fig 4.2.2 Predicted effect of E_e on PV module I based on performance model.....	19
Figure 4.3.1 PV module Electrical Performance Simulator.....	21
Solar Declination for the month of January.....	40
Solar Declination for the month of June.....	40
Solar Declination for the month of November.....	41

List of Appendices

Appendix A.....39

Appendix B.....40

Chapter 1

Introduction

1.1 Objective and Motivation

The objective of this project is to determine the effects of mounting orientation (i.e. mounting angle on top of a building roof) of a photovoltaic panel on power output. Based on the simulation results, the report proposes an alternative energy management technique to characterize the unstable nature of the photovoltaic power generating system. Energy-efficiency practices are becoming essential as energy prices continue to rise and the impacts of climate change emerge. Institutions that adopt measures to reduce energy and the associated greenhouse gas emissions will acquire financial, environmental and social benefits. One way to ease the financial encumbrance of increasing energy price instability is to reduce dependence on electricity, propane, oil and natural gas by switching to emerging renewable energy sources, including solar energy (direct, passive and active), wind, biomass, micro-hydro and geothermal (heat from the ground). Renewable energy is promptly available and, once capital costs are incurred, it is ultimately free. Systems may stand alone, i.e., off the utility grid, or be inter-tied (connected) to the grid. In Canada, large-scale hydro-electricity constitutes the bulk of the renewable energy supply. However, significant opportunities exist by using emerging renewable energy technologies to reduce the load on the already existed electrical network [1].

A typical power generating system using photovoltaic technology would have many components. These components include: Solar cell array subsystem, orientation subsystem, power collection subsystem, energy storage subsystem, power regulating subsystem, power distribution subsystem, and finally end users. The software used for this study is the PV-DesignPro. This software is designed to simulate photovoltaic energy system operation on an hourly basis for one year, based on a user selected climate and system design. Its built-in databases of common equipment and user-oriented interface will make it possible to reach a new level of PV design conception and performance maximization. PV systems are far too expensive to rely on simple sizing

methods, where unneeded over-design of modules or batteries could cost thousands of extra dollars.

1.2 Background

Solar energy is a renewable resource that is environmentally friendly. Unlike fossil fuels, solar energy is available just about everywhere on earth. This source of energy is free, immune to rising energy prices. Solar energy can be used in many ways - to provide heat, lighting, mechanical power and electricity.

The photovoltaic effect was first described by French physicist Edmond Becquerel in 1839, but it remained a curiosity of science for the next three-quarters of a century. Becquerel found that certain materials would produce small amounts of electric current when exposed to light. The effect was first studied in solids by Heinrich Hertz in the 1870s. Shortly afterward, selenium photovoltaic cells were converting light to electricity at 1% to 2% efficiency. Selenium was quickly adopted in the emerging field of photography for use in light-measuring devices. Major steps toward commercializing PV were taken in the 1940s and early 1950s when the Czochralski process for producing highly pure crystalline silicon was developed. In 1954, scientists at Bell Laboratories depended on the Czochralski process to develop the first crystalline silicon photovoltaic cell, which had an efficiency of 4%.

Although little attempts were made in the 1950s to use silicon cells in commercial products, it was the space program that gave the technology its first major application. In 1958, the U.S. Vanguard space satellite carried a small array of PV cells to power its radio. The cells performed so well that PV technology has been part of the space program ever since. Today, solar cells power virtually all satellites, including those used for communications, defense, and scientific research. The US space shuttle fleet uses PV arrays to generate much of its electrical power [4].

The computer industry, especially transistor semiconductor technology, also contributed to the development of PV cells. Transistors and PV cells are made from similar materials and operate on the basis of similar physical mechanisms. Advances in transistor research have provided a continuous flow of new information about PV cell technology. Today, however, this technology transfer process often works in reverse, as advances in PV

research and development are sometimes adopted by the semiconductor industry. Despite these advances, photovoltaic systems in 1970 were still too expensive for most terrestrial uses. The rising energy costs sparked by oil prices in the mid-1970s renewed interest in making PV technology more affordable. Since then, the federal government, industry, and research organizations have invested hundreds of millions of dollars in research, development, and production. Often, industry and the federal government work together, sharing the cost of PV research and development. Much of this effort has gone into the development of crystalline silicon, the material Bell's scientists used to make the first practical cells. As a result, crystalline silicon devices have become more and more efficient, reliable, and durable. Industry and government have also explored a number of other promising materials, such as non-crystalline (amorphous) silicon, polycrystalline cadmium telluride and copper indium diselenide, and other single crystal materials like gallium arsenide. Today's commercial PV systems can convert from 5% to 15% of sunlight into electricity. They are highly reliable, and they last 20 years or longer.

1.3 General Approach to the Problem

In order to achieve the objective of this Master of Engineering project, it was necessary to understand the characteristics of the simulator used to study the photovoltaic systems. Without this understanding, it would be impossible to analyze the results obtained from the simulator. However, the simulator is just an analytical tool. Without a complete understanding of the performance of photovoltaic systems, it would be very difficult to judge the reliability of the results obtained from the simulator. Therefore, the study of the simulator and its governing equations was followed by a thorough research on PV systems. This research is shown in the literature part of this report. Once the literature review had been completed, the simulator was used. The PV-DesignPro can be used to evaluate PV system designs more effectively than current worksheet based methods. In addition, it is an in-depth learning tool that produces information on likely PV system performance ever possible. Its built-in databases of common equipment and user-oriented interface make it possible to reach a new level of PV design conception and performance maximization. PV systems are far too expensive to rely on simple sizing methods, where unneeded over-design of modules or batteries could cost thousands of extra dollars.

Appropriate software has been long needed in this area to solve difficult questions on intelligent system design and configuration. The following steps are followed when simulating the performance of the designed PV array:

1. Load a sample PV system file.
2. Choose a climate.
3. Adjust the Load.
4. Choose a Wiring Configuration.
5. AC Inverter.
6. Calculate the Results for the System.

The starting point for any simulation is the inputs, and any PV system simulation has several primary inputs that are limited by accuracy:

1. The PV module test results input parameters.
2. System load inputs.
3. The climate data.
4. The mathematical models used in the simulation.

Every effort has been made to stretch the limits of accuracy while maintaining reasonableness and quickness in the simulation. However it should be advised that:

1. PV module testing data is lightly available best, and manufacturers have been known to provide skewed data in certain cases. Organizations such as Sandia National Labs and the Florida Solar Energy Center are working on module test databases that will be available to the public soon. This type of independent, standardized data will increase the utility of the program results.
2. System loads in most systems will fluctuate dramatically from a set schedule of weekdays and weekends. A residential household is a good example, and demonstrates the difficulty of determining the exact nature of the proposed load for one year into the future.
3. Climates will fluctuate and change dramatically from an annual average that is taken from 30 years of data (such as in TMY2 data).
4. The mathematical models used in the simulation, despite being based on some of the best available information, are merely simplifications of what happens in nature. It would

be difficult for a 3-10 second calculation to model many of the physics related intricacies of PV module operation that are unnecessary in estimating annual performance.

As a result, no simulation despite detail or complexity can propose 100% accuracy. The simulation is a best effort design measure. It should be understood annual results can fluctuate dramatically based on the above factors from what is derived using the simulation.

Chapter 2

Current Photovoltaic Technology Assessment

The literature relating to photovoltaic (PV) and its applications is vast. However, there is little literature that is directly related to the objective of this project which is determining the effects of PV module mounting angle on its power output. This was a motivation to proceed with this project and investigate the effects of the PV module mounting angle on power output even further.

Literature was drawn from various aspects of the project such as effects of rising temperature on photovoltaic panel output and effects of irradiance levels during different year's months on panel output. The goal of the literature review was to understand the application and operation of photovoltaic systems in order to interpret simulator results correctly.

2.0 PV Array System

A solar cell array can be thought of as a system that is composed of a number of subsystems, as shown in Fig. 2.0.1. The optical subsystem includes sunlight concentrators and the solar cell or array cover glass. All solar cells and their wiring form the electrical subsystem. The solar cell mechanical support constitutes the mechanical subsystem, and the structural supports and sun-tracking mechanisms are parts of the orientation and structural subsystem. Array temperature transducers, orientation sensors, voltage and current transducers, and other status or performance monitoring devices are accounted for with their circuits, by the status sensor subsystem. The thermal control subsystem is comprised of heat radiators, cooling fins, thermal control coatings, and other items that reduce the solar cell operating temperature as much as is practical. Solar cell packaging material represents the environmental protection subsystem that minimizes adverse environmental effects on the solar cells [1].

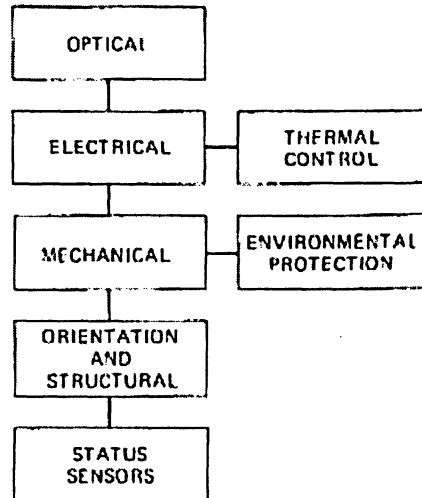


Fig 2.0.1 The subsystem of an array

2.1 Current-Voltage Characteristics

Current-voltage characteristics, or, in brief, I—V curves, describe the solar cell electrical terminal characteristics most completely. A solar cell I—V curve passes through three significant points:

1. I_{SC} , short-circuit current where cell terminal voltage is zero;
2. P_{mp} , maximum power output point, also known as the optimum power output point, P_{op} and
3. V_{OC} , open-circuit voltage where cell terminal current is zero.

The maximum power point, ' P_{mp} ' corresponds to the maximum conversion efficiency, this point is located where the rectangle having the largest area can be drawn inside the I—V curve. The I-V curve is tangent to a constant power curve, also called an iso-efficiency curve at the P_{mp} point at which $dP/dV = 0$ (Fig. 2.1.1b). From a set of several constant efficiency curves drawn on the I-V curve plot, the actual cell operating efficiency can be determined when the cell is operated off the maximum power point (i.e., when the terminal voltage $V \neq V_{mp}$).[1]

Corresponding to " P_{mp} " there is an optimum power current, ' I_{mp} ' and a optimum or maximum power voltage, V_{mp} . A straight line drawn from the origin through P_{mp} (Fig. 2.1.1a) represents the optimum load resistance, R_{Lopt} , for this cell. The slope of this line is $1/R_{Lopt} = I_{mp}/V_{mp}$.

Frequently, the values for P_{mp} , V_{mp} , and I_{mp} are determined from experimentally obtained I-V curves. As seen from Fig. 2.1.1a, the point of tangency of the I-V curve and a constant power curve is not sharply defined; as an aid to more closely defining the ' P_{mp} ' point, a P-V curve, as shown in Fig. 2.1.1b, can be constructed. P-V curves can be plotted during the solar cell test when I—V curves are taken or they can be computer-generated from I-V curve data. The I-V curve shown in Fig. 2.1.1 is only the first quadrant portion of the entire I-V curve. In general, the I—V curve extends from the second quadrant through the first quadrant into the fourth quadrant.

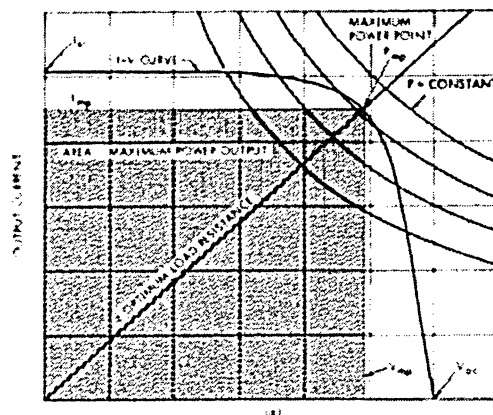


Fig 2.1.1a Solar cell electrical output characteristics;
(a) I-V Curve.

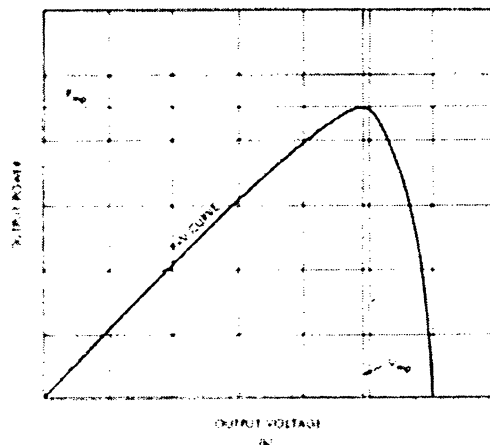


Fig2.1 1b Solar cell electrical output characteristics;
(b) P-V Curve.

Sometimes the I—V curve is shown rotated such that I is plotted on the abscissa and V on the ordinate. Such presentation is logical and correct except it is not conventional according to the solar cell theoretical model, in which output current is the dependent

variable which usually is plotted on the ordinate. (Actually, the nomenclature “I—V” curve is reversed.) Sometimes the photovoltaic portion of the I-V curve is shown “upside down” in the fourth quadrant. Such representation, while logically self-consistent, is inconsistent with modern circuit analysis techniques and leads to unnecessary conceptual difficulties, such as negative power output.

Another reason for showing the output current as negative arises from the solution of the so-called continuity equation which assigns a negative sign to the cell current. This calculated cell current is an internal cell current which must flow in a certain direction to maintain the conservation of electrical charges. According to modern circuit theory when this internal cell current flows in an outside circuit, the “sign” of it reverses and it flows identically to the conventional current, from a higher to a lower potential. [2]

2.2 Reversible Effects of Temperature

A change in cell temperature causes three changes in the cell I-V curve, two of which are clearly evident in Fig. 2.2.1:

1. A scaling of the I-V curve along the current axis;
2. A shifting of the I-V curve along the voltage axis; and
3. A change in the I-V curve shape affecting the “roundness” of the “knee” region of the I-V curve.

An increase in the cell operating temperature causes a slight increase in the cell short-circuit current and a significant decrease in cell voltage. The increase in short-circuit current is a function of illumination level. Its value, typically less than 0.1%/°C, depends upon the spectral distribution of the illuminating light (filtered sunlight) and the spectral response of the solar cells (i.e., the cell thickness, junction depth, anti-reflective coating, and state of radiation damage of the cell).

Scaling of the I-V curve along the current axis corresponds to a change in the cell’s energy conversion efficiency, which, in turn, is due to a change in the cell’s collection efficiency with temperature. Scaling of the I-V curve consists of multiplication of the value of the output current at each point on the I-V curve by a constant; for an increase in temperature, this constant is greater than unity and for a decrease in temperature, it is less than unity. [3]

The change in voltage with temperature is due to a change in the diode conduction characteristics. With increasing temperatures, the entire I—V curve translates toward lower voltages at a rate of approximately 2.2 to 2.3 mV/°C. This voltage change is almost the same for all non-irradiated, thick base width solar cells (for V_{oc} and V_{mp}), as well as for general rectifier diodes made from silicon.

With elevated temperatures, the “knee” region of the I—V curve tends to become more rounded. This “knee softening” can be accommodated analytically by either using separate temperature coefficients for I_{sc} , I_{mp} , V_{mp} , and V_{oc} , by defining a temperature coefficient for R_s , or by defining a separate “curve rounding” factor. Differences between the temperature coefficients of V_{oc} , and V_{mp} are usually indicative of changes in the I-V curve shape with temperature.

With increasing temperature, the cell’s reverse saturation current increases in the same way the reverse current of conventional diodes increases. However, this increase in true reverse current is usually not observable because it is masked by the much larger solar cell leakage currents. Cell leakage currents do not have well-defined temperature dependence. In the avalanche breakdown region, solar cells usually show decreasing breakdown voltages with increasing temperatures.[1]

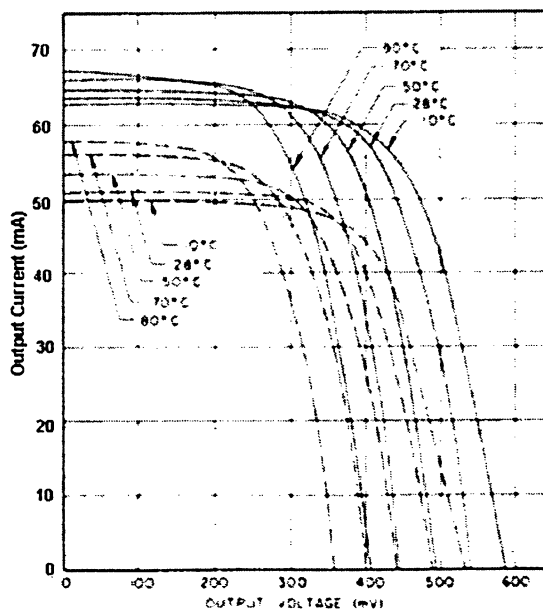


Fig2.2.1 Typical variations of solar cell current- voltage characteristics with temperature before (solid lines) and after (dashed lines) irradiation.

Chapter 3

Statement of Problem and Methodology of Solution

3.1 Statement of Problem

Electricity has become a major part of our daily lives. With high oil prices driving energy prices up, photovoltaic systems and other reusable energy sources are becoming more needed. However, a better understanding of the unstable nature of photovoltaic systems is crucial in order to maximize the power output of these systems. Such an understanding would result in a more affordable alternative energy source to the end user. In addition, an understanding of the unstable nature of PV systems would ultimately result in systems that are more environments friendly. The problem lays in the fact that climate, which plays a major part in the power output of the PV panels, is unpredictable and uncontrollable. Thus it became necessary for research to be conducted in order to characterize the unstable nature of PV systems. In particular, an understanding of the effect of the mounting angle of the PV module on power output became crucial in order to maximize the power output of the module. The study would have to reveal the advantage, if any, of a sun-tracking PV module over a fixed module. In particular, the study should answer the following questions: Should a PV panel be placed at 90 deg to the building roof? Is a mounting angle of 40 deg. better than a 55 deg? Do the changing seasons have an effect on the PV module power output irrespective of the module mounting angle?

One way to ease the financial burden of increasing energy price instability is to reduce dependence on electricity, propane, oil and natural gas by switching to emerging renewable energy sources such as solar energy, wind, biomass, and geothermal. Renewable energy is readily available and it is virtually free. Systems may stand alone, i.e., off the utility grid, or be inter-tied to the grid. In Canada, large-scale hydro-electricity constitutes the body of the renewable energy supply. However, significant opportunities exist by using emerging renewable energy technologies. [5]

3.2 Solution Methodology

A considerable amount of time was spent in order to arrive to a point where the design process could begin. Literature review covered various topics such as the solar cell polarity, I-V curves, series resistance, shunt resistance, and effects of temperature variation on PV module power output. The flowchart below outlines the basic approach to solving the problem at hand.

As illustrated in the flowchart, the project started by researching various topics related to PV modules electrical performance. This included familiarization with the function of photovoltaic panels. This was a necessary step, as it provided the background information for successful analyzing of simulation results. The next step consisted of actual design. The design process was tedious as it was accompanied by research. The design difficulty lay in the fact that it could not be verified in the lab. In addition, the simulator does not provide the capability of distinguishing between the output results. There are two main inputs to the simulator. These are the climate data for the city of Toronto averaged over the last 30 years and the desired PV module mounting angle. Based on these inputs, the simulator outputs the expected irradiance value taking into account the sun position as well as the time equation calculated for the city of Toronto. Although the simulator calculated the expected power output of a PV module corresponding to a particular module mounting angle, it did not offer the means to determine the optimum module mounting angle. As a result, it was decided to run the simulations for four predetermined module mounting angles. These angles are 0, 30, 60, and 90 degrees respectively. The 0 deg mounting angle corresponds to a PV module that is placed horizontally parallel to the roof surface. The 90 deg mounting angle corresponds to a PV module placed perpendicular to the building roof facing the sun. Next, four days of the month corresponding to the beginning of each week within a particular month were chosen to run the simulations. This was necessary in order to capture the change in the PV module power output with respect to the time of month at a specific module mounting angle. Further, in order to characterize the change in PV module power output with respect to the time of day, the simulations were run for four different hours of the day. Many alternative designs were produced in order to determine the optimum mounting angle of a photovoltaic module. In addition, designs were

produced for systems with 100% connected electrical building load. Other designs did not account for any connected load. It simply assumed a grid-connected PV system where all energy produced is fed back into the grid for a possible credit. It was ultimately decided to run the simulations for a system with no electrical connected load. After enough research was completed, alternative designs were produced, however, only the most cost effective solution is to be implemented in hardware. As each of these designs was completed, they were simulated to ensure proper operation. As the simulation results were obtained, modifications were made as necessary to obtain desired results. Once the simulations were successful, the project was deemed complete. One of the major difficulties encountered during the design is that simulations could not be verified in the lab. Therefore, the literature review which is part of this report was extremely helpful. The solution methodology is shown in the flow chart below:

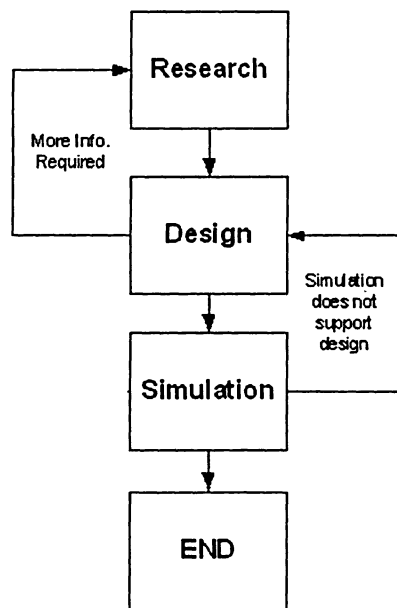


Figure 3.2.1 Solution Methodology Flowchart

Chapter 4

Simulation of PV Module Mounting Angle

In order to arrive to a functional and accurate product a number of design considerations are required. In an engineering design, one must define a problem, generate alternative solutions, evaluate these alternatives, and finally choose a particular solution. As was mentioned earlier, this project two components. The first component was to determine the optimum mounting angle for the PV module in order to maximize the module output. This chapter answers this question based on the simulation results. The detailed description of the photovoltaic module and array performance model developed and used in the simulator is explained below. The performance model can be used in several different ways. It can be used to design a photovoltaic array for a given application based on expected power and energy production on an hourly, monthly, or annual basis [9]. It can be used to determine an array power rating by translating measured parameters to performance at a standard reference condition. In addition, it can be used to monitor the actual versus predicted array performance over the life of the photovoltaic system. The performance model is empirically based; however, it achieves its flexibility and accuracy from the fact that individual equations used in the model are derived from individual solar cell characteristics. The effect of the solar irradiance on the PV module performance model was investigated mathematically as shown in the equations below. This effect was used later in the simulator to determine the optimum mounting angle for a PV module that would maximize the PV module power output. The findings are shown and explained below.

4.1 PV MODULE PERFORMANCE MODEL USED IN THE SIMULATOR

The objective of any testing and modeling effort is usually to quantify and replicate the measured phenomenon of interest. Testing and modeling PV module performance in the outdoor environment is typically complicated by the influences of a variety of interactive

factors related to the environment and solar cell physics. In order to effectively design, implement, and monitor the performance of photovoltaic systems, a performance model must be able to separate and quantify the influence of all significant factors.

The following equations define the model used in the Simulator in order to model the performance of photovoltaic modules. The equations depict the electrical performance for individual PV modules, and can be scaled for any number of series or parallel combination of modules in an array.

The form of the model given by Equations (1) through (10) is used to when calculating the expected power and energy produced by a module, assuming that predetermined module performance coefficients and solar resource information are available. The solar resource and weather data required by the model can be obtained from tabulated databases recorded by the National Weather agency or from direct measurements. The three classic points on a module current-voltage (I-V) curve, short-circuit current, open-circuit voltage, and the maximum-power point, are given by the first four equations.

$$I_{sc} = I_{SCO} \cdot f_1(A_{Ma}) \cdot \{(E_b \cdot f_2(AOI) + f_d \cdot E_{diff}) / E_o\} \cdot \{1 + \alpha_{Isc} \cdot (T_c - T_o)\} \quad (1)$$

$$I_{mp} = I_{mpo} \cdot \{C_o \cdot E_e + C_1 \cdot E_e^2\} \cdot \{1 + \alpha_{Imp} \cdot (T_c - T_o)\} \quad (2)$$

$$V_{oc} = V_{OCO} + N_s \cdot \delta(T_c) \cdot \ln(E_e) + \beta_{Voc}(E_e) \cdot (T_c - T_o) \quad (3)$$

$$V_{mp} = V_{mpo} + C_2 \cdot N_s \cdot \delta(T_c) \cdot \ln(E_e) + C_3 \cdot N_s \cdot \{\delta(T_c) \cdot \ln(E_e)\}^2 + \beta_{Vmp}(E_e) \cdot (T_c - T_o) \quad (4)$$

$$P_{mp} = I_{mp} \cdot V_{mp} \quad (5)$$

$$FF = P_{mp} / (I_{sc} \cdot V_{oc}) \quad (6)$$

where:

$$E_e = I_{sc} / [I_{SCO} \cdot \{1 + \alpha_{Isc} \cdot (T_c - T_o)\}] \quad (7)$$

$$\delta(T_c) = n \cdot k \cdot (T_c + 273.15) / q \quad (8)$$

The ‘effective’ solar irradiance describes the fraction of the total solar irradiance incident on the module to which the cells inside actually respond. It is defined in equation (7). When tabulated solar resource data are used in predicting module performance, Equation (7) is used directly.

The two additional points on the I-V curve are given by Equations (9) and (10). The fourth point (I_x) is given at a voltage equal to one-half of the open-circuit voltage, and the fifth (I_{xx}) at a voltage midway between V_{mp} and V_{oc} . The five points provided by

the performance model provide the basic shape of the I-V curve and can be used to regenerate a close approximation to the entire I-V curve in cases where an operating voltage other than the maximum-power-voltage is required.

$$I_x = I_{xo} \cdot \{ C_4 \cdot E_e + C_5 \cdot E_e^2 \} \cdot \{ 1 + (\alpha_{Isc}) \cdot (T_c - T_o) \} \quad (9)$$

$$I_{xx} = I_{xxo} \cdot \{ C_6 \cdot E_e + C_7 \cdot E_e^2 \} \cdot \{ 1 + (\alpha_{Imp}) \cdot (T_c - T_o) \} \quad (10)$$

Where:

I_{sc} = Short-circuit current (A)

I_{mp} = Current at the maximum-power point (A)

I_x = Current at module $V = 0.5 \cdot V_{oc}$

I_{xx} = Current at module $V = 0.5 \cdot (V_{oc} + V_{mp})$

V_{oc} = Open-circuit voltage (V)

V_{mp} = Voltage at maximum-power point (V)

P_{mp} = Power at maximum-power point (W)

FF = Fill Factor (dimensionless)

N_s = Number of cells in series in a module's cell-string

N_p = Number of cell-strings in parallel in module

k = Boltzmann's constant, 1.38066E-23 (J/K)

q = Elementary charge, 1.60218E-19 (coulomb)

T_c = Cell temperature inside module (°C)

δ(T_c) = 'Thermal voltage' per cell at temperature T_c, approximately 1 volt for a typical 36-cell crystalline silicon module

E_e = The 'effective' solar irradiance

C₀, C₁ = empirically determined coefficients relating I_{mp} to effective irradiance, E_e. C₀+C₁ = 1, (dimensionless)

C₂, C₃ = empirically determined coefficients relating V_{mp} to effective irradiance (C₂ is

Dimensionless, and C3 has units of 1/V)

C4, C5 = empirically determined coefficients relating the current (I_x), to effective irradiance, E_e . $C4+C5 = 1$, (dimensionless)

C6, C7 = empirically determined coefficients relating the current (I_{xx}) to effective irradiance, E_e . $C6+C7 = 1$, (dimensionless)

n = empirically determined 'diode factor' associated with individual cells in the module, (dimensionless). It is determined using measurements of V_{oc} translated to a common temperature and plotted versus the natural logarithm of effective irradiance. This Relationship is typically linear over a wide range of irradiance (~ 0.1 to 1.4 suns).

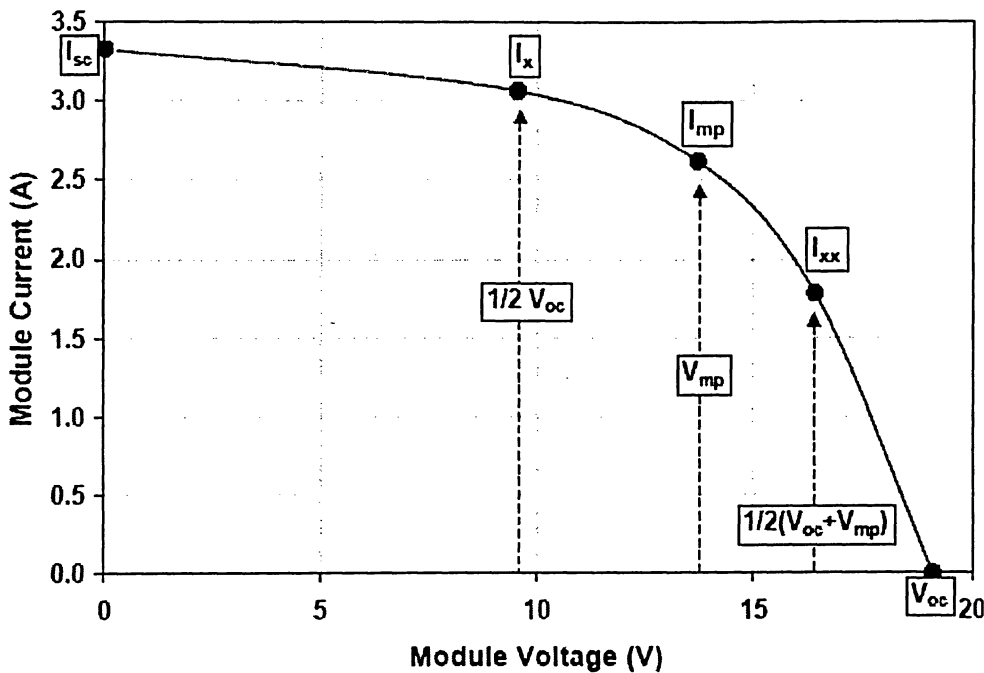


Fig4.1.1 I-V curve reconstructed using the module performance model used in the simulator

Equations (1) through (10) can also be used for arrays of modules by simply accounting for the series and parallel combinations of modules in the array. If the number of modules connected in series in a module-string is M_s then the voltages calculated using Equations (3) and (4) should be multiplied by M_s . If the number of module-strings connected in parallel in the array is M_p then the currents calculated using Equations (1), (2), (9), and (10) should be multiplied by M_p .

Ideally, performance (I-V) measurements at the array level are available, in which case the accuracy of the performance model can be further improved. Array measurements can provide the four basic performance parameters (I_{sco} , I_{mpo} , V_{oco} , V_{mpo}) at the standard reference condition, as well as the eight other coefficients (C_0 , C_1 , ..., C_7). The spectral influence, $f_1(AMa)$, the optical losses, $f_2(AOI)$, and the temperature coefficients for the array are assumed to be available from test results on individual modules.[16] In this situation, the electrical performance of the entire array can be modeled completely, and the model directly includes the array-level losses associated with module mismatch and wiring resistance. In essence, the array is modeled as if it were a very large module.

4.2 EFFECT OF IRRADIANCE (W/M^2) ON PV MODULE PERFORMANCE MODEL

The following module performance parameters relate the PV module's voltage and current, and as a result the shape of the I-V curve (fill factor), to the solar irradiance level. Figure 4.2.1 demonstrates how the measured values for module V_{mp} and V_{oc} may vary as a function of the effective irradiance. The measured values were translated to a common temperature ($50^\circ C$) in order to remove temperature dependence.

The coefficients (n , C_2 , C_3) were obtained using regression analyses based on Equations (3) and (4). The coefficients were then used in the performance model to calculate voltage versus irradiance behaviour at different operating temperatures. Figure 4.2.2 illustrates how the measured values for module current (I_{sc} , I_{mp} , I_x , I_{xx}) may vary as a function of the effective irradiance. Similar to the voltage analysis, the measured current values were translated to a common temperature to remove temperature dependence. The performance coefficients (C_0 , C_1 , C_4 , C_5 , C_6 , C_7) associated with I_{mp} , I_x , and I_{xx} were then determined using regression analyses based on Equations (2), (9), and (10). The formulation of the performance model uses the complexity associated with Equation (1) to account for any 'non-linear' behaviour associated with I_{sc} . As a result, the plot of I_{sc} versus the 'effective irradiance' variable is always linear.

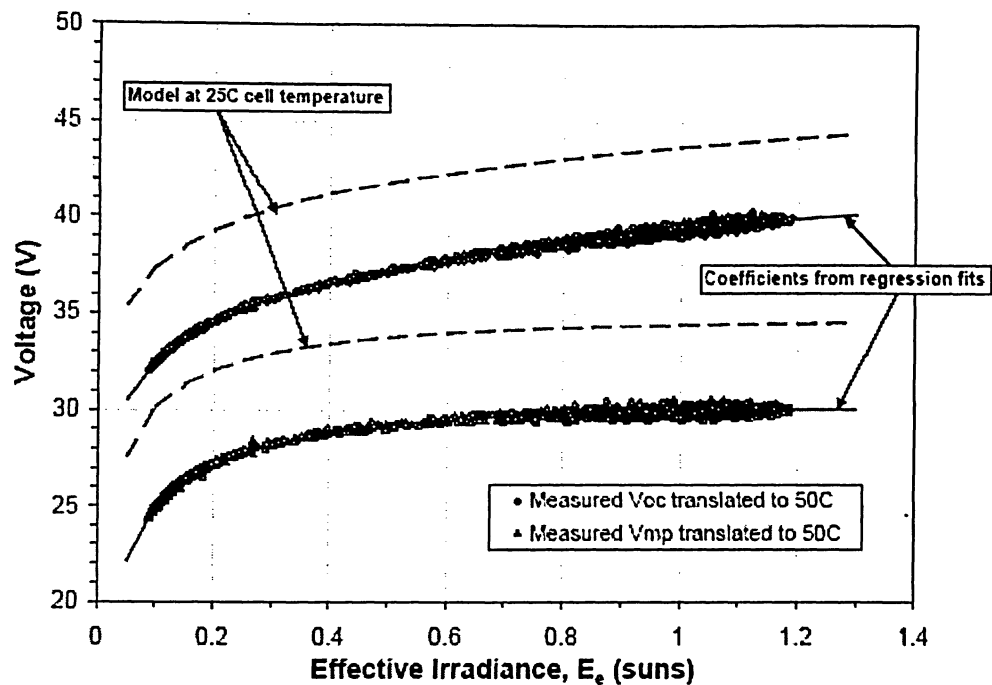


Fig 4.2.1 Predicted effect of E_e on PV module voltage based on performance model. Measured values for V_{oc} and V_{mp} were translated to a common temperature, 50°C . Performance model provides the predicted curves at 25°C .

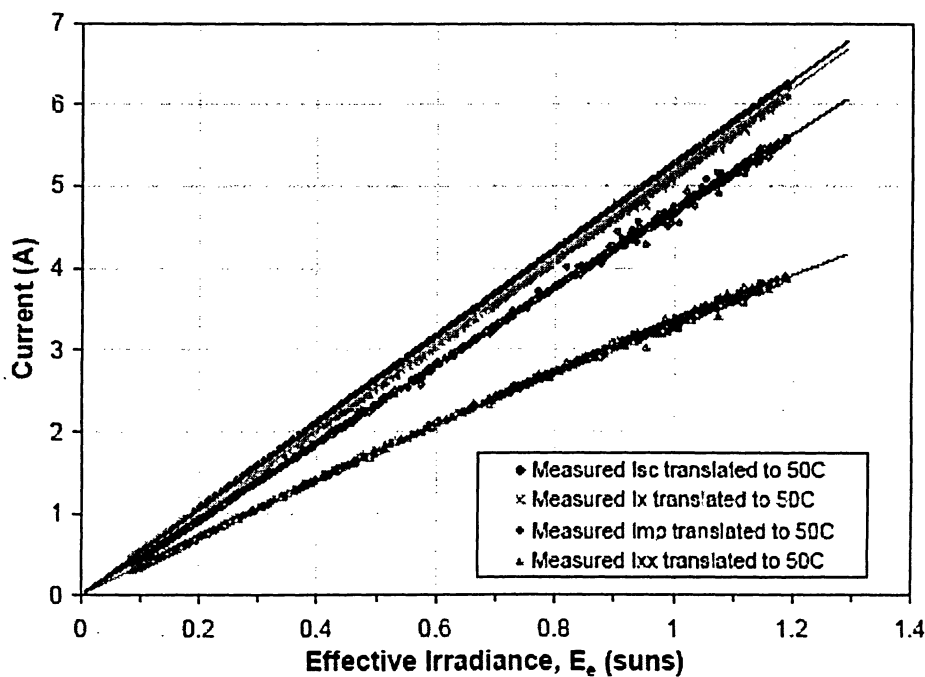


Fig 4.2.2 Predicted effect of E_e on PV module I based on performance model. Measured values for currents were translated to a common temperature, 50°C , prior to regression analysis.

The empirical functions $f_1(\text{AMa})$ and $f_2(\text{AOI})$ are used in the performance model to account for the influence on PV module short-circuit current due to variation in the solar spectrum and the optical losses due to solar angle-of-incidence. These functions are determined by a module testing laboratory using explicit outdoor test procedures [10, 15]. The intent of these two functions is to account for systematic effects that occur on a continuing basis during the predominantly clear conditions when the majority of solar energy is collected. For crystalline silicon modules, the normalized I_{sc} is typically several percent higher at high air mass conditions than it is at solar noon. For practical purposes, the effects of intermittent clouds, smoke, dust, and other conditions can be considered random influences that average out on a weekly, monthly, or annual basis.

The influence of the changing solar spectrum is relatively small for air mass values between 1 and 2. In the context of annual energy production, it should also be recognized that over 90% of the solar energy available over an entire year occurs at air mass values less than 3. So, the spectral influence illustrated at air mass values higher than 3 is of somewhat academic importance for the system designer. As documented elsewhere [9], the cumulative affect of the solar spectral influence on annual energy production is typically quite small, less than 3%.

Standard Reporting Conditions are used by the photovoltaic industry to specify the performance of the module. This rating is provided at a single standardized (reference) operating condition [16]. The associated performance parameters are typically either manufacturer's nameplate ratings or test results obtained from a module testing laboratory. The accuracy of these performance specifications is critical to the design of photovoltaic arrays and systems because they provide the reference point from which performance at all other operating conditions is derived. The performance parameters and conditions associated with the standard reporting condition are defined as follows:

T_o = Reference cell temperature for rating performance, typically 25°C

I_{sco} = $I_{sc}(E = E_o \text{ W/m}^2, \text{AMa} = 1.5, T_c = T_o \text{ }^\circ\text{C}, \text{AOI} = 0^\circ)$ (A)

I_{mpo} = $I_{mp}(E_e = 1, T_c = T_o)$ (A)

V_{oco} = $V_{oc}(E_e = 1, T_c = T_o)$ (V)

$$V_{mpo} = V_{mp}(E_e=1, T_c = T_o) \text{ (V)}$$

$$I_{xo} = I_x(E_e=1, T_c = T_o) \text{ (A)}$$

$$I_{xxo} = I_{xx}(E_e=1, T_c = T_o) \text{ (A)}$$

As explained above, solar irradiance has a direct effect on determining the shape of the PV module I-V curve. Therefore, it was determined to use this effect along with the module performance model shown above in order to determine the effect of the PV module mounting angle on power output. This in addition to the simulation results are shown below.

4.3 Photovoltaic (PV) Simulator

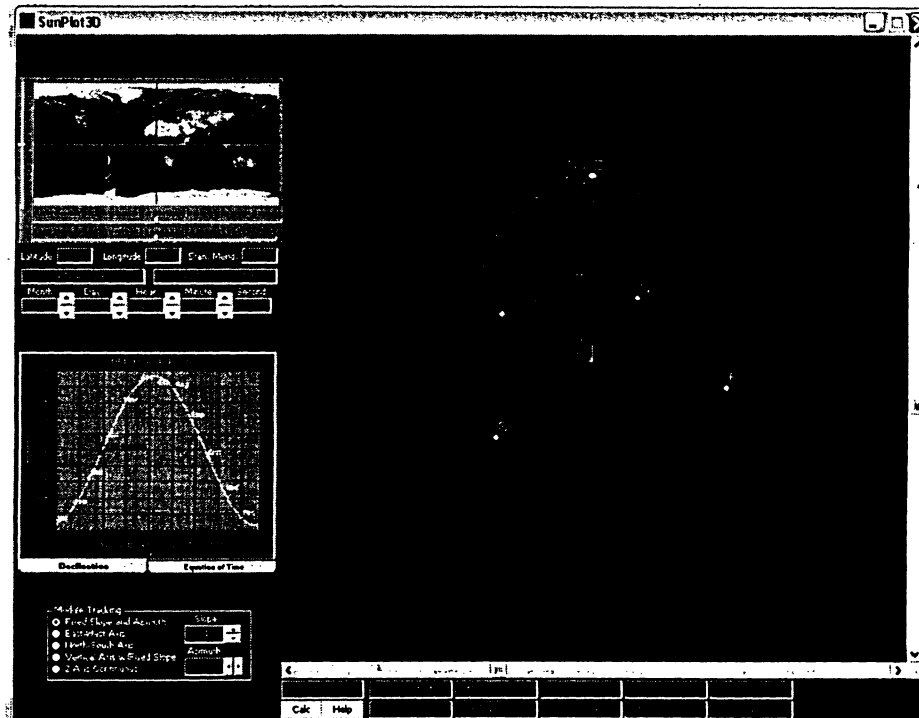


Figure 4.3.1 PV module Electrical Performance Simulator

The simulator was designed to be an effective tool to investigate the characteristics and electrical performance of PV modules.

At the top left corner of the simulator screen, there is a map of the world. On this map, there are 3 kinds of axis. First, there is the yellow axis which is used to enter the value of

the Latitude of a certain location or city. Second is the red axis, which enables the user to enter the Longitude value of a certain location on the world map. Finally, the green axis calculates the Standard Meridian based on a certain values of Latitude and Longitude. Below these boxes are selection buttons that allow the user to enter the month of year, the day of month, the hour of the days, the minute of the hour, and finally for more accuracy the seconds of the minute. These entries are based on user design requirements. Specifying these values, would allow the user to document the change in sun position and as a result the effect on the solar module power output based on the time of year.

For the purpose of this project, the simulator was used to determine the effect of PV module mounting angle on module's power output. Toronto is located at Latitude of 43.4 deg and a Longitude of 79.20 deg.

The simulator offers the capability of simulating PV module power output based on various sun tracking methods. For example, the solar module tracking method could be specified to have a fixed slope and Azimuth. The fixed slope means the fixed angle that the module is mounted at with respect to a flat surface (Earth). The Azimuth means the angle of the solar module off of south. Further, the simulator allows the user to specify the sun tracking method as either East/West or North/South. This means that the program would allow the user to simulate the change in PV module power output as it tracks the position of the sun during the time of day. For the purpose of this project, it was assumed that the tracking method for the proposed installation in the City of Toronto is going to be of fixed slope and Azimuth. Using the simulator it is evident to the user that in the city of Toronto, the sun always rises in the Southern hemisphere. This means that during the design process, the proposed array of solar modules to be installed would have to be facing south in order to maximize the module's exposure to the sun beam irradiation.

The simulator allows the user to investigate various PV module electrical characteristics such as: DECLINATION, ZENITH ANGLE, SOLAR ALTITUDE, SOLAR AZIMUTH, AIRMASS, MODULE SLOPE, MODULE AZIMUTH, ANGLE OF INCIDENCE, RATIO OF BEAM RAD. (R_b), TOTAL HORIZONTAL

IRRADIATION (W/m^2) (H-Irr), MODULE IRRADIATION (W/m^2) (M-Irr), and finally, the STANDARD MERIDIAN. As was explained in section 4.2, the effect of solar irradiance on PV module performance model was used in order to determine the PV module's optimum mounting angle. The MODULE IRRADIATION (W/m^2) (M-Irr) value refers to the Solar radiation on the tilted module surface calculated using the Perez model. The RATIO OF BEAM RAD. (Rb) value refers to the ratio of beam radiation on the tilted module surface to that on a horizontal surface. In particular, the M-Irr value was used to determine the optimum module mounting angle based on the module performance model used in the simulator.

4.4 Simulation Results for the City of Toronto

One of the limitations of the simulator is that it does not calculate the optimum module mounting angle automatically. In addition, it does not organize the simulated results into a form that allows comparison between output results. Therefore, in order to determine the optimum module mounting angle, it was necessary to tabulate the results obtained from the simulator into a form that allows comparison between the various results. The various developed tables are shown below. Each table documents the simulated results for a specific module mounting angle. In order to increase the accuracy and the reliability of the comparisons between the simulated results, it was decided to tabulate the change in PV module power characteristics for four different days of the month. Furthermore, the simulated results reveal the effect of the sun's position in Toronto at different hours of the day on the PV module power output.

The tables were organized in such a way as to ease the comparison between the different results obtained for the different module mounting angles.

		MODULE SLOPE = 0/ MODULE AZM=0																			
		7TH DAY				16TH DAY				23RD DAY				30TH DAY				AVERAGE			
		HOUR				HOUR				HOUR				HOUR				HOUR			
		9	12	3	6	9	12	3	6	9	12	3	6	9	12	3	6	9	12	3	6
JAN	H-IRR W/M	131	340	152	0	132	340	164	0	143	361	186	0	160	391	213	0				
	M-IRR W/M	131	340	152	0	132	340	164	0	143	361	186	0	160	391	213	0	141.5	358	178.8	0
	RB	1	1	1	1	1	1	1	1	1	1	1	1	1	1	1	1				
FEB	H-IRR W/M	194	446	257	0	224	475	285	0	252	505	313	0	286	541	345	0				
	M-IRR W/M	194	446	257	0	224	475	285	0	252	505	313	0	286	541	345	0	239	491.8	300	0
	RB	1	1	1	1	1	1	1	1	1	1	1	1	1	1	1	1				
MAR	H-IRR W/M	322	583	376	0	371	634	421	0	421	687	462	11	472	737	500	24				
	M-IRR W/M	322	583	376		371	634	421		421	687	462	11	472	737	500	24	396.5	660.3	439.7	17.5
	RB	1	1	1	1	1	1	1	1	1	1	1	1	1	1	1	1				
APR	H-IRR W/M	517	772	527	39	536	774	538	55	575	812	571	71	615	853	606	89				
	M-IRR W/M	517	772	527	39	536	774	538	55	575	812	571	71	615	853	606	89	560.7	802.7	560.5	63.5
	RB	1	1	1	1	1	1	1	1	1	1	1	1	1	1	1	1				
MAY	H-IRR W/M	651	889	637	108	663	887	639	125	665	884	644	139	667	886	653	152				
	M-IRR W/M	651	889	637	108	663	887	639	125	665	884	644	139	667	886	653	152	661.5	886.5	643.2	131
	RB	1	1	1	1	1	1	1	1	1	1	1	1	1	1	1	1				
JUN	H-IRR W/M	690	920	688	173	714	984	712	187	700	932	703	189	682	913	693	189				
	M-IRR W/M	690	920	688	173	714	984	712	187	700	932	703	189	682	913	693	189	696.5	937.3	699	184.5
	RB	1	1	1	1	1	1	1	1	1	1	1	1	1	1	1	1				
JULY	H-IRR W/M	665	898	684	186	683	937	717	190	680	939	714	180	667	926	698	165				
	M-IRR W/M	665	898	684	186	683	937	717	190	680	939	714	180	667	926	698	165	673.7	925	703.3	180.3
	RB	1	1	1	1	1	1	1	1	1	1	1	1	1	1	1	1				
AUG	H-IRR W/M	623	871	647	136	598	851	625	111	590	845	608	89	576	830	582	65				
	M-IRR W/M	623	871	647	136	598	851	625	111	590	845	608	89	576	830	582	65	596.7	849.3	615.5	100.3
	RB	1	1	1	1	1	1	1	1	1	1	1	1	1	1	1	1				
SEP	H-IRR W/M	543	785	529	38	483	708	458	11	461	683	424	0	439	657	389	0				
	M-IRR W/M	543	785	529	38	483	708	458	11	461	683	424	0	439	657	389	0	481.5	708.3	450	19.5
	RB	1	1	1	1	1	1	1	1	1	1	1	1	1	1	1	1				
OCT	H-IRR W/M	414	627	352	0	360	555	287	0	183	506	247	0	286	465	214	0				
	M-IRR W/M	414	627	352	0	360	555	287	0	183	506	247	0	286	465	214	0	310.8	538.3	275	0
	RB	1	1	1	1	1	1	1	1	1	1	1	1	1	1	1	1				
NOV	H-IRR W/M	258	440	190	0	226	407	163	0	196	372	144	0	171	343	130	0				
	M-IRR W/M	258	440	190	0	226	407	163	0	196	372	144	0	171	343	130	0	212.8	390.5	156.8	0
	RB	1	1	1	1	1	1	1	1	1	1	1	1	1	1	1	1				
DEC	H-IRR W/M	150	323	121	0	139	326	125	0	131	324	128	0	126	324	133	0				
	M-IRR W/M	150	323	121	0	139	326	125	0	131	324	128	0	126	324	133	0	136.5	324.3	126.8	0
	RB	1	1	1	1	1	1	1	1	1	1	1	1	1	1	1	1				

Table 4.4.1 Simulation results for module slope at 0 Deg

		MODULE SLOPE = 30/ MODULE AZM=0																AVERAGE			
		7TH DAY				16TH DAY				23RD DAY				30TH DAY							
		HOUR				HOUR				HOUR				HOUR				HOUR			
		9	12	3	6	9	12	3	6	9	12	3	6	9	12	3	6	9	12	3	6
JAN	H-IRR W/M'	131	340	152		132	340	164		143	361	186		160	391	213		290.5	645	356	0
	M-IRR W/M'	280	637	323	0	278	622	336	0	291	644	365	0	313	677	400	0				
	RB	2.61	1.96	2.47	0	2.48	1.90	2.30	0.2	2.35	1.84	2.17	0.16	2.20	1.78	2.03	0.1				
FEB	H-IRR W/M'	194	446	257	0	224	475	285	0	252	505	313	0	286	541	345	0	398.7	769.7	490.7	0
	M-IRR W/M'	357	741	456	0	385	757	479	0	411	777	501	0	442	804	527	0				
	RB	2.02	1.70	1.89	0.03	1.84	1.62	1.75	0	1.71	1.55	1.65	0	1.60	1.49	1.56	0				
MAR	H-IRR W/M'	322	583	376	0	371	634	421	0	421	687	462	11	472	737	500	24	542	896.5	600.2	15
	M-IRR W/M'	480	846	556	0	520	872	586	0	564	915	617	11	604	953	642	19				
	RB	1.52	1.45	1.50	0	1.41	1.38	1.4	0	1.34	1.34	1.34	1.41	1.28	1.29	1.28	0.66				
APR	H-IRR W/M'	517	772	527	39	536	774	538	55	575	812	571	71	615	853	606	89	651.5	961.7	650.2	38.5
	M-IRR W/M'	635	966	648	27	631	937	633	35	657	959	650	42	683	985	670	50				
	RB	1.22	1.25	1.22	0.43	1.16	1.2	1.16	0.32	1.12	1.17	1.12	0.29	1.09	1.14	1.08	0.27				
MAY	H-IRR W/M'	651	889	637	108	663	887	639	125	665	884	644	139	667	886	653	152	691.5	977.7	669.5	67.5
	M-IRR W/M'	703	1007	687	58	697	983	668	64	687	965	661	71	679	956	662	77				
	RB	1.06	1.12	1.05	0.27	1.03	1.09	1.02	0.27	1.01	1.08	1	0.28	0.99	1.06	0.99	0.30				
JUN	H-IRR W/M'	690	920	688	173	714	984	712	187	700	932	703	189	682	913	693	189	693	986	697	96.2
	M-IRR W/M'	693	983	690	88	710	1006	708	97	694	987	699	99	675	968	691	101				
	RB	0.98	1.05	0.98	0.31	0.97	1.05	0.97	0.33	0.97	1.04	0.97	0.35	0.97	1.04	0.97	0.37				
JULY	H-IRR W/M'	665	898	684	186	683	937	717	190	680	939	714	180	667	926	698	165	681.7	1000	719	102.7
	M-IRR W/M'	661	956	686	102	686	1006	727	107	691	1019	734	104	689	1019	729	98				
	RB	0.97	1.05	1.33	0.36	0.98	1.06	0.99	0.40	0.99	1.07	1.01	0.4	1.01	1.09	1.02	0.41				
AUG	H-IRR W/M'	623	871	647	136	598	851	625	111	590	845	608	89	576	830	582	65	663.2	985.2	687	62.5
	M-IRR W/M'	662	976	691	83	656	977	690	69	665	991	689	56	670	997	678	42				
	RB	1.04	1.11	1.05	0.41	1.51	1.14	1.08	0.41	1.11	1.16	1.11	0.39	1.14	1.19	1.15	0.35				
SEP	H-IRR W/M'	543	785	529	38	483	708	458	11	461	683	424	0	439	657	389	0	620.2	918.5	579	14
	M-IRR W/M'	657	970	639	23	613	908	581	5	608	901	559	0	603	895	537	0				
	RB	1.19	1.23	1.19	0.25	1.26	1.28	1.26	0	1.32	1.32	1.32	1.68	1.38	1.37	1.39	0.89				
OCT	H-IRR W/M'	414	627	352	0	360	555	287	0	183	506	247	0	286	465	214	0	533.5	808.5	431.2	0
	M-IRR W/M'	595	891	509	0	548	824	444	0	512	778	403	0	478	741	369	0				
	RB	1.45	1.42	1.47	0.73	1.55	1.49	1.6	0.65	1.64	1.55	1.71	0.61	1.74	1.62	1.84	0.57				
NOV	H-IRR W/M'	258	440	190	0	226	407	163	0	196	372	144	0	171	343	130	0	401.5	681	305.5	0
	M-IRR W/M'	454	728	340	0	422	704	319	0	383	664	293	0	347	628	270	0				
	RB	1.87	1.69	2.01	0.54	2.02	1.78	2.21	0.5	2.15	1.84	2.36	0.47	2.29	1.9	2.5	0.45				
DEC	H-IRR W/M'	150	323	121	0	139	326	125	0	131	324	128	0	126	324	133	0	286.7	610.7	273.7	0
	M-IRR W/M'	316	603	260	0	289	619	273	0	276	611	276	0	266	610	286	0				
	RB	2.42	1.95	2.61	0.41	2.62	1.99	2.68	0.37	2.72	2.03	2.72	0.34	2.76	2.03	2.67	0.3				

Table 4.4.2 Simulation results for module slope at 30 Deg

		MODULE SLOPE = 60/ MODULE AZM=0																			
		7TH DAY				16TH DAY				23RD DAY				30TH DAY				AVERAGE			
		HOUR				HOUR				HOUR				HOUR				HOUR			
		9	12	3	6	9	12	3	6	9	12	3	6	9	12	3	6	9	12	3	6
JAN	H-IRR W/M ²	131	340	152		132	340	164		143	361	186		160	391	213		310.2	764	486.5	0
	M-IRR W/M ²	308	768	457	0	297	741	465	0	308	759	494	0	328	788	530	0				
	RB	3.97	2.44	3.15	0	3.69	2.33	2.89	0	3.39	2.23	2.68	0	3.06	2.11	2.47	0				
FEB	H-IRR W/M ²	194	446	257	0	224	475	285	0	252	505	313	0	286	541	345	0				
	M-IRR W/M ²	377	845	587	0	400	844	596	0	420	851	607	0	443	864	621	0	410	851	602.7	0
	RB	2.69	1.98	2.24	0	2.31	1.82	2.01	0	2.05	1.71	1.84	0	1.82	1.6	1.69	0				
MAR	H-IRR W/M ²	322	583	376	0	371	634	421	0	421	687	462	11	472	737	500	24	558.7	917.2	617.2	12.5
	M-IRR W/M ²	524	904	602	0	545	901	611	0	572	924	625	12	594	940	631	13				
	RB	1.64	1.51	1.60	0	1.45	1.40	1.43	0	1.32	1.31	1.31	1.44	1.21	1.24	1.21	0.14				
APR	H-IRR W/M ²	517	772	527	39	536	774	538	55	575	812	571	71	615	853	606	89	588.5	891.5	586.2	26.2
	M-IRR W/M ²	603	929	615	18	577	876	578	24	583	878	576	29	591	883	576	34				
	RB	1.11	1.16	1.11	0	1.01	1.08	1	0	0.94	1.03	0.93	0	0.89	0.98	0.87	0				
MAY	H-IRR W/M ²	651	889	637	108	663	887	639	125	665	884	644	139	667	886	653	152	560.7	837	539.7	43.2
	M-IRR W/M ²	591	885	575	38	569	845	541	44	549	818	526	45	534	800	517	46				
	RB	0.84	0.94	0.82	0	0.78	0.90	0.77	0	0.75	0.87	0.74	0	0.72	0.84	0.71	0				
JUN	H-IRR W/M ²	690	920	688	173	714	984	712	187	700	932	703	189	682	913	693	189	530.2	810.5	534	51.2
	M-IRR W/M ²	536	813	532	50	543	826	541	52	528	809	534	52	514	794	529	51				
	RB	0.70	0.82	0.69	0	0.68	0.81	0.68	0	0.67	0.81	0.68	0	0.67	0.81	0.68	0				
JULY	H-IRR W/M ²	665	898	684	186	683	937	717	190	680	939	714	180	667	926	698	165	532.5	838.2	568	51.5
	M-IRR W/M ²	505	788	530	51	531	838	569	53	543	857	583	52	551	870	590	50				
	RB	0.68	0.82	0.69	0	0.70	0.83	0.72	0	0.72	0.86	0.74	0	0.75	0.88	0.77	0				
AUG	H-IRR W/M ²	623	871	647	136	598	851	625	111	590	845	608	89	576	830	582	65	573	886	596.2	36.5
	M-IRR W/M ²	545	849	573	45	559	870	592	39	583	900	606	34	605	925	614	28				
	RB	0.79	0.92	0.81	0	0.86	0.97	0.87	0	0.91	1.01	0.92	0	0.98	1.06	0.99	0				
SEP	H-IRR W/M ²	543	785	529	38	483	708	458	11	461	683	424	0	439	657	389	0	611.2	909	570.2	11.5
	M-IRR W/M ²	615	924	598	18	597	890	565	5	610	904	561	0	623	918	557	0				
	RB	1.07	1.13	1.07	0	1.18	1.22	1.18	0	1.28	1.29	1.28	1.91	1.39	1.37	1.40	0.53				
OCT	H-IRR W/M ²	414	627	352	0	360	555	287	0	183	506	247	0	286	465	214	0				
	M-IRR W/M ²	634	939	545	0	606	893	495	0	580	861	463	0	555	836	436	0	593.7	882.2	484.7	0
	RB	1.51	1.46	1.55	0.27	1.69	1.58	1.76	0.12	1.85	1.69	1.96	0.05	2.02	1.80	2.19	0				
NOV	H-IRR W/M ²	258	440	190	0	226	407	163	0	196	372	144	0	171	343	130	0				
	M-IRR W/M ²	542	838	423	0	517	829	398	0	478	793	373	0	439	759	347	0	494	804.7	385.2	0
	RB	2.23	1.93	2.48	0	2.50	2.08	2.82	0	2.73	2.19	3.09	0	2.96	2.29	3.33	0				
DEC	H-IRR W/M ²	150	323	121	0	139	326	125	0	131	324	128	0	126	324	133	0				
	M-IRR W/M ²	407	736	337	0	394	761	356	0	373	762	366	0	361	761	377	0	383.7	755	359	0
	RB	3.19	2.38	3.51	0	3.45	2.45	3.64	0	3.59	2.48	3.64	0	3.67	2.48	3.56	0				

Table 4.4.3 Simulation results for module slope at 60 Deg

		MODULE SLOPE = 90/ MODULE AZM=0																			
		7TH DAY				16TH DAY				23RD DAY				30TH DAY				AVERAGE			
		HOUR				HOUR				HOUR				HOUR				HOUR			
		9	12	3	6	9	12	3	6	9	12	3	6	9	12	3	6	9	12	3	6
JAN	HJRR WM ²	131	340	152	0	132	340	164	0	143	361	186	0	160	391	213	0				
	MJRR WM ²	358	726	408	0	352	695	413	0	359	704	435	0	374	721	461	0	360.7	711.5	429.2	0
	RB	3.49	2.19	3.21	0	3.23	2.07	2.87	0	2.96	1.95	2.6	0	2.68	1.83	2.34	0				
FEB	HJRR WM ²	194	446	257	0	224	475	285	0	252	505	313	0	286	541	345	0				
	MJRR WM ²	407	760	503	0	414	741	499	0	419	732	498	0	425	726	496	0	416.2	739.7	499	0
	RB	2.31	1.67	2.05	0	1.94	1.50	1.77	0	1.68	1.37	1.57	0	1.46	1.25	1.38	0				
MAR	HJRR WM ²	322	583	376	0	371	634	421	0	421	687	462	11	472	737	500	24				
	MJRR WM ²	441	740	503	0	439	712	490	0	444	711	484	10	443	703	470	10	441.7	716.5	486.7	10
	RB	1.31	1.17	1.27	0	1.09	1.04	1.07	0	0.95	0.94	0.94	1.09	0.82	0.85	0.82	0				
APR	HJRR WM ²	517	772	527	39	536	774	538	55	575	812	571	71	615	853	606	89				
	MJRR WM ²	429	671	437	16	388	608	388	22	374	590	368	27	361	574	350	31	388	610.7	385.7	24
	RB	0.70	0.76	0.70	0	0.59	0.67	0.58	0	0.51	0.61	0.50	0	0.44	0.56	0.43	0				
MAY	HJRR WM ²	651	889	637	108	663	887	639	125	665	884	644	139	667	886	653	152				
	MJRR WM ²	345	557	332	36	314	511	294	39	290	481	273	44	271	459	259	47	305	502	289.5	41.5
	RB	0.39	0.51	0.37	0	0.33	0.46	0.31	0	0.29	0.42	0.27	0	0.26	0.40	0.24	0				
JUN	HJRR WM ²	690	920	688	173	714	984	712	187	700	932	703	189	682	913	693	189				
	MJRR WM ²	261	456	257	51	256	456	256	53	246	445	252	53	240	438	252	53	250.7	448.7	254.2	52.5
	RB	0.23	0.37	0.22	0	0.21	0.36	0.21	0	0.20	0.36	0.21	0	0.20	0.36	0.21	0				
JULY	HJRR WM ²	665	898	684	186	683	937	717	190	680	939	714	180	667	926	698	165				
	MJRR WM ²	239	438	257	52	259	476	286	54	275	498	303	53	292	519	320	50	266.2	482.7	291.5	52.2
	RB	0.21	0.37	0.22	0	0.23	0.39	0.25	0	0.25	0.41	0.28	0	0.29	0.44	0.31	0				
AUG	HJRR WM ²	623	871	647	136	598	851	625	111	590	845	608	89	576	830	582	65				
	MJRR WM ²	304	524	327	44	333	560	357	36	366	598	384	31	400	635	406	25	350.7	579.2	368.5	34
	RB	0.34	0.48	0.36	0	0.41	0.54	0.43	0	0.48	0.59	0.49	0	0.56	0.65	0.56	0				
SEP	HJRR WM ²	543	785	529	38	483	708	458	11	461	683	424	0	439	657	389	0				
	MJRR WM ²	428	658	417	16	440	659	416	5	467	689	431	0	495	720	444	0	457.5	681.5	427	10.5
	RB	0.66	0.73	0.66	0	0.79	0.83	0.78	0	0.90	0.91	0.90	1.62	1.03	1	1.04	0.04				
OCT	HJRR WM ²	414	627	352	0	360	555	287	0	183	506	247	0	286	465	214	0				
	MJRR WM ²	519	757	450	0	515	742	427	0	507	732	411	0	496	725	397	0	509.2	739	421.2	0
	RB	1.17	1.11	1.21	0	1.37	1.25	1.46	0	1.55	1.37	1.69	0	1.75	1.50	1.95	0				
NOV	HJRR WM ²	258	440	190	0	226	407	163	0	196	372	144	0	171	343	130	0				
	MJRR WM ²	496	742	395	0	485	749	381	0	455	725	362	0	424	702	339	0	465	729.5	369.2	0
	RB	2	1.65	2.28	0	2.31	1.82	2.68	0	2.57	1.95	2.99	0	2.84	2.07	3.26	0				
DEC	HJRR WM ²	150	323	121	0	139	326	125	0	131	324	128	0	126	324	133	0				
	MJRR WM ²	397	685	332	0	389	713	353	0	368	716	362	0	357	715	372	0	377.7	529	354.7	0
	RB	3.10	2.17	3.48	0	3.40	2.26	3.63	0	3.57	2.29	3.63	0	3.57	2.29	3.63	0				

Table 4.4.4 Simulation results for module slope at 90 Deg

4.5 Discussion

The effect of solar irradiance on PV module performance model was used in the simulator in order to determine the effect of PV module mounting angle on power output. For the purpose of this project, it was assumed that the tracking method for the proposed installation in the City of Toronto is going to be of fixed slope and Azimuth. The City of Toronto is located at Latitude of 43.4 deg and a Longitude of 79.20 deg. Using the simulator it is evident to the user that in the city of Toronto the sun always rises in the Southern hemisphere. This means that during the design process the proposed array of

		0 deg slope				30 deg slope			
		AVERAGE				AVERAGE			
		HOUR				HOUR			
		9	12	3	6	9	12	3	6
JAN	M-IRR W/M	141.5	358	178.8	0	290.5	645	356	0
FEB	M-IRR W/M	239	491.8	300	0	398.7	769.7	490.7	0
MAR	M-IRR W/M	396.5	60.3	439.7	17.5	542	896.5	600.2	15
APR	M-IRR W/M	560.7	802.7	560.5	63.5	651.5	961.7	650.2	38.5
MAY	M-IRR W/M	661.5	886.5	643.2	131	691.5	977.7	669.5	67.5
JUN	M-IRR W/M	696.5	937.3	699	184.5	693	986	697	96.2
JULY	M-IRR W/M	673.7	925	703.3	180.3	681.7	1000	719	102.7
AUG	M-IRR W/M	596.7	849.3	615.5	100.3	663.2	885.2	687	62.5
SEPT	M-IRR W/M	481.5	708.3	450	19.5	620.2	818.5	579	14
OCT	M-IRR W/M	310.8	538.3	275	0	533.5	808.5	431.2	0
NOV	M-IRR W/M	212.8	390.5	156.8	0	401.5	681	305.5	0
DEC	M-IRR W/M	136.5	24.3	126.8	0	286.7	510.7	273.7	0

Table 4.5.1 0 deg vs. 30 comparisons

solar modules to be installed in Toronto would have to be facing south, so as to maximize the module's exposure to the sun beam irradiation.

Comparing the solar irradiance measurements for PV module mounting angles of 0 deg and 30 deg, it is evident that at 9 am, a module slope of 30 deg would produce better M-Irr values than those of a 0 slope installation. At noon, a 30 deg slope produces better results than those obtained at noon time for a 0 deg slope with peak values during the months of June and July. At a 30 deg mounting slope, the M-Irr values for the months of June and July were 986 and 1000 W/m² respectively. At 3pm, a 30 deg mounting slope results still produced better results, with peak values of 697 and 719 w/m² for the months of June and July respectively. The lowest values were observed to be for the months of

		90 deg slope				30 deg slope			
		AVERAGE				AVERAGE			
		HOUR				HOUR			
		9	12	3	6	9	12	3	6
JAN	M-IRR W/M	360.7	711.5	429.2	0	290.5	645	356	0
FEB	M-IRR W/M	416.2	739.7	499	0	398.7	769.7	490.7	0
MAR	M-IRR W/M	441.7	716.5	486.7	10	542	896.5	500.2	15
APR	M-IRR W/M	388	610.7	385.7	24	651.5	961.7	550.2	38.5
MAY	M-IRR W/M	305	502	289.5	41.5	691.5	977.7	669.5	67.5
JUN	M-IRR W/M	250.7	448.7	254.2	52.5	693	986	697	96.2
JUL	M-IRR W/M	266.2	482.7	291.5	52.2	681.7	1000	719	102.7
AUG	M-IRR W/M	350.7	579.2	368.5	34	663.2	985.2	687	62.5
SEP	M-IRR W/M	457.5	681.5	427	10.5	620.2	918.5	579	14
OCT	M-IRR W/M	509.2	739	421.2	0	533.5	808.5	431.2	0
NOV	M-IRR W/M	465	729.5	369.2	0	401.5	681	305.5	0
DEC	M-IRR W/M	377.7	529	354.7	0	286.7	510.7	273.7	0

Table 4.5.2 90 deg vs. 30 comparisons

November and December which still were better than those obtained for a 0 deg slope for the same months. At 6pm, the 0 deg slope chart revealed an over all better w/m^2 results than those obtained for the 30 deg mounting slope. In general, the above results revealed that an installation based on a module slope of 30 deg would be more beneficial in terms of w/m^2 than that of a 0 deg slope.

Comparing the solar irradiation simulation results for mounting angles of 30 deg and 60 deg, it is evident that at 9 am, a module slope of 30 deg would produce better M-Irr values than those of a 60 deg slope installation for the months between April and September. From September to March, the 60 deg module slope produced results that

		90 deg slope				60 deg slope			
		AVERAGE				AVERAGE			
		HOUR				HOUR			
		9	12	3	6	9	12	3	6
JAN	M IRR W/M	360.7	711.5	429.2	0	310.2	764	486.5	0
FEB	M IRR W/M	416.2	739.7	499	0	410	851	602.7	0
MAR	M IRR W/M	441.7	716.5	486.7	10	558.7	917.2	517.2	12.5
APR	M IRR W/M	388	610.7	385.7	24	588.5	891.5	586.2	26.2
MAY	M IRR W/M	305	502	289.5	41.5	560.7	837	539.7	43.2
JUN	M IRR W/M	250.7	448.7	254.2	52.5	530.2	810.5	534	51.2
JULY	M IRR W/M	266.2	482.7	291.5	52.2	532.5	838.2	568	51.5
AUG	M IRR W/M	350.7	579.2	368.5	34	573	886	596.2	36.5
SEPT	M IRR W/M	457.5	681.5	427	10.5	611.2	909	570.2	11.5
OCT	M IRR W/M	509.2	739	421.2	0	593.7	882.2	484.7	0
NOV	M IRR W/M	465	729.5	369.2	0	494	804.7	385.2	0
DEC	M IRR W/M	377.7	529	354.7	0	383.7	755	359	0

Table 4.5.3 90 deg vs. 60 comparisons

were slightly better than those of the 30 deg mounting slope. At noon time, similar results were observed. A 30 deg slope produces better results for the months between April and September, while a 60 deg slope had better results for the months between September and March. Similar results were observed for 3 pm and 6 pm. These results can be explained using the solar declination charts shown in Appendix B. The solar declination chart shows that during the months between April and September, the solar declination is high and of positive value. This means that a slightly tilted solar module, such as 30 deg, would be subjected to higher M-Irr value as supposed to a module with a sharper slope such as 60 deg. On the other hand, the solar declination chart shows a

		30 deg slope				60 deg slope			
		AVERAGE				AVERAGE			
		HOUR				HOUR			
		9	12	3	6	9	12	3	6
JAN	M-IRR W/M	290.5	645	356	0	310.2	764	486.5	0
FEB	M-IRR W/M	398.7	769.7	490.7	0	410	851	602.7	0
MAR	M-IRR W/M	542	896.5	600.2	15	558.7	917.2	617.2	12.5
APR	M-IRR W/M	651.5	961.7	650.2	38.5	588.5	991.5	686.2	26.2
MAY	M-IRR W/M	691.5	977.7	669.5	67.5	560.7	837	539.7	43.2
JUN	M-IRR W/M	693	986	697	96.2	530.2	810.5	534	51.2
JULY	M-IRR W/M	681.7	1000	719	102.7	532.5	838.2	568	51.5
AUG	M-IRR W/M	663.2	985.2	687	62.5	573	886	596.2	36.5
SEP	M-IRR W/M	620.2	918.5	579	14	611.2	909	570.2	11.5
OCT	M-IRR W/M	533.5	808.5	431.2	0	593.7	882.2	484.7	0
NOV	M-IRR W/M	401.5	681	305.5	0	494	804.7	385.2	0
DEC	M-IRR W/M	286.7	510.7	273.7	0	383.7	755	359	0

Table 4.5.4 30 deg vs. 60 comparisons

negative value corresponding to a lower declination between September and March. This means that the sun would be rising and setting at an angle close to the earth surface, resulting in better M-Irr values for the sharper module mounting angles, such as 60 deg. Based on the above results, if it is a design requirement to maximize the PV system output during the summer time, a module slope of 30 deg would be preferred. On the other hand, if a maximum PV-system output is desired during the winter time then a mounting slope of 60 deg is preferred. It is worth mentioning that these simulated values are based on ideal conditions. Given the barbarous Canadian weather during winter, it is safe to assume that maximizing the PV power generating system output during the

summer time would be more beneficial than winter based PV system. This is due to the fact that during winter time (September to March) the PV-system would be subjected to an increased number of limiting factors such as long periods of snow, rain, and clouds. As a result, the M-Irr values shown in the simulation results would be driven even lower.

Comparing the w/m^2 results obtained for the 30 deg module slope with those of the 90 deg module slope, it is evident that the w/m^2 results for 30 deg module slope are significantly better. Comparing the w/m^2 results obtained for the 60 deg module slope with those of the 90 deg slope; it is evident that the power output for the 60 deg module slope is significantly better for most months.

Based on the above power output comparisons, it is safe to assume that PV module mounting angles of 30 and 60 deg would significantly improve the performance of the PV power generating system.

4.6 Energy Management

Although this study attempted to determine the effect of PV module mounting angle on power output, it should be noted that the nature of PV systems is unstable. This is due to the fact that PV modules produce energy from sunrays, which is an uncontrollable source. In addition, climate interference is a major concern. Any changes to the weather conditions would significantly affect the PV module output. Therefore, along with optimizing the PV system design, the designer should attempt incorporating energy management techniques in his/her design in order to reduce the demand load on the system.

One of the more difficult areas of design is to obtain suitable interfaces between the application devices, such as motors, heating units, and other utilization devices, and the relatively low-energy control systems. The interfacing of remote control systems and application devices requires careful coordination between the mechanical equipment or motor control center, manufacturer, and the manufacturer of the supervisory control equipment. One major problem is the compatibility of control devices, the controlled equipment, and the signal system.

When information is transmitted to remote power equipment, these should be checked to find out if they have functioned as required. It is desired to know if someone turned the lights on in a local area, or if a piece of equipment was started locally without computer or other automatic control intervention. Therefore, feedback from the controlled areas or equipment to the motor control center is desirable.

Some energy conservation devices and concepts that may be utilized are listed below. Some are basically energy demand reduction devices, while others are more concerned with overall energy conservation.

- 1) Load limiters are devices that are programmed to operate building loads in sequence or in a way such that the billing demand remains at an optimized value. These devices can be used to provide alarms when the rate of energy usage exceeds established levels.
- 2) Use of automated devices for shutting down or reducing the level of operation of nonessential equipment. In terms of lighting, typically the illumination levels would be reduced to 50%. Variable speed equipment with feedback control can materially reduce energy requirements. This can be combined with other simple devices, such as photocell, infrared, or ultrasonic control of lighting, and then integrated with the computerized controls of the heating and ventilating system.
- 3) Use of waste heat, including that from lighting fixtures, as part of the space-conditioning system.
- 4) Energy can be recovered in vertical transportation equipment by utilizing regenerative systems. A descending elevator, for example, can feed back energy into the power system.
- 5) Use of high-efficiency motors, drives, belts, and power factor correcting ballasts will minimize line and equipment losses. Power factor correcting equipment (i.e., capacitors, synchronous motors) and the proper sizing of induction motors will serve to maintain the facility power factor at high values with minimum losses. [7]

Control over a building's energy usage (kWh) and the rate of its usage (kW) should always be attempted in order to reduce the load on any environmentally friendly power generating systems. The simple fact that no energy is used when equipment is shut off should always be utilized.

Early demand controllers were tied into a meter-pulse system and began shutting down equipment when it appeared that a preset demand would be exceeded. While this procedure can significantly reduce electric costs, there is some question as to the amount of energy saved (or added). A second generation of controllers has increased the effectiveness of this system by shedding or delaying operation of all nonessential loads in addition to keeping the demand under a preset level.

It is important to establish the existing pattern of electrical usage and to identify those areas where energy consumption could be reduced. A month-by-month record of electricity usage is available from electric bills, and this usage should be carefully recorded in a format that will ease future reference, evaluation, and analysis. The following list of items should be recorded in the electric usage history:

- 1) Billing month
- 2) Reading data
- 3) Days in billing cycle
- 4) Kilowatt-hours
- 5) Billing kW demand (or kVA demand, if billed on this basis)
- 6) Actual kW demand (or kVA demand, if billed on this basis)
- 7) Kilovats (actual and billed)
- 8) Kilovar hours (actual and billed)
- 9) Power factor (average or peak, as billed)
- 10) Load factor (average use compared to peak use)
- 11) Power bill (broken down into the above categories along with fuel cost)
- 12) Occupancy level
- 13) Heating or cooling degree days
- 14) A electricity usage history, including appropriate remarks (such as vacation periods)

A listing of building operations, equipment, and energy conservation opportunities (ECOs) will also provide both a usage history and a basis for evaluating future improvement. The listing of this information, along with electricity usage, is part of the energy audit. In general, there are four categories of ECOs. These four categories are as follows:

- 1) Housekeeping Measures. These include easily performed actions such as turning lights off when not required; cleaning or changing air filters; cleaning heat exchangers; keeping doors shut; and turning off redundant motors, pumps, and fans.
- 2) Equipment Modification. This is usually more difficult and more expensive because it involves physical changes to the electric system. Examples include the addition of solid-

state, adjustable speed drives; reducing motor sizes on existing equipment; removing light fixtures; adding automatic controls to reduce lighting in unoccupied areas; and modifying heating and cooling systems.

3) Better Equipment Utilization such as the use of natural lighting as much as possible. Others include the redirection of warmer air to cooler parts of the building during the heating season, and prioritizing starting times for tenants to reduce energy demand or consumption, or both.

4) Changes to the Building Shell. Simple improvements to the insulation quality of the building reduce energy losses to the outside environment significantly. Changes to the building shell could be as simple as adding insulation, reducing infiltration, controlling exhaust/intake and reducing heat gains in the inside environment by using reflective materials, shading, and insulation.

Housekeeping and low-cost means should be undertaken without delay. The larger and more expensive ECOs generally take longer to initiate and should often be performed after low-cost measures are completed. However, there may be cases when obvious equipment modification improvements can be made concurrently with low-cost improvements.

Finally, the unstable nature of PV systems can be compensated for by the addition of a wind turbine system. For critical loads, an emergency power supply line can be incorporated in the design in order ensure availability of uninterruptible power when needed. With the addition of a PV system, the emergency supply line can be undersized reducing the cost of material (i.e. copper and insulation).

Chapter 5

Conclusion

The effect of solar irradiance on PV module performance model was used in order to determine the effect of PV module mounting angle on module power output. The performance model can be used in several different ways. It can be used to design a photovoltaic array for a given application based on expected power and energy production on an hourly, monthly, or annual basis [9]. It can be used to determine an array power rating by translating measured parameters to performance at a standard reference condition. In addition, it can be used to monitor the actual versus predicted array performance over the life of the photovoltaic system. The performance model is empirically based; however, it achieves its flexibility and accuracy from the fact that individual equations used in the model are derived from individual solar cell characteristics.

Equations (1) through (10) given in chapter 4 can be used for arrays of modules by simply accounting for the series and parallel combinations of modules in the array. If the number of modules connected in series in a module-string is M_s then the voltages calculated using Equations (3) and (4) should be multiplied by M_s . If the number of module-strings connected in parallel in the array is M_p then the currents calculated using Equations (1), (2), (9), and (10) should be multiplied by M_p . The calculated array performance using this approach is based on the expected performance of the individual modules, and as a result may be slightly optimistic because other array-level losses such as module mismatch and wiring resistance are not included.

Based on the simulation results presented in chapter 4, it is evident that a PV module mounting angle of 30 deg would produce better M-Irr values for the months between April and September; while a PV module mounting angle of 60 deg would optimize the PV power system output for the months between September and March. The simulation results can be explained using the solar declination charts shown in Appendix B. The solar declination charts show that during the months between April and September, the solar declination is high with positive value. On the other hand, between the months of September and March the solar declination is low with a negative value. Based on the

findings of this report, if it is a design requirement to maximize the PV system power output during the summer time, a module slope of 30 deg would be preferred. However, if a maximum PV-system power output is desired during the winter time then a PV mounting angle of 60 deg would be preferred. It is worth mentioning that the simulation results are based on ideal conditions. In addition, the findings of this report were based on a PV system with fixed azimuth.

The empirical functions $f_1(\text{AMa})$ and $f_2(\text{AOI})$ discussed in chapter four are used in the performance model to account for the influence on PV module short-circuit current due to variation in the solar spectrum and the optical losses due to solar angle-of-incidence. These functions are determined by a module testing laboratory using explicit outdoor test procedures [10, 15].

The results of this report can be further improved by incorporating a sun tracking mechanism into the PV system. The consequence of a 10% error in the module performance rating will be a 10% effect on the annual energy production from the photovoltaic system. System integrators and module manufacturers should make every effort to ensure the accuracy of module performance ratings.

Given the barbarous Canadian weather during the winter time, it is safe to assume that maximizing the PV- system power output during the Summer months would produce better economic return for a grid connected photovoltaic system.

5.1 Recommendations

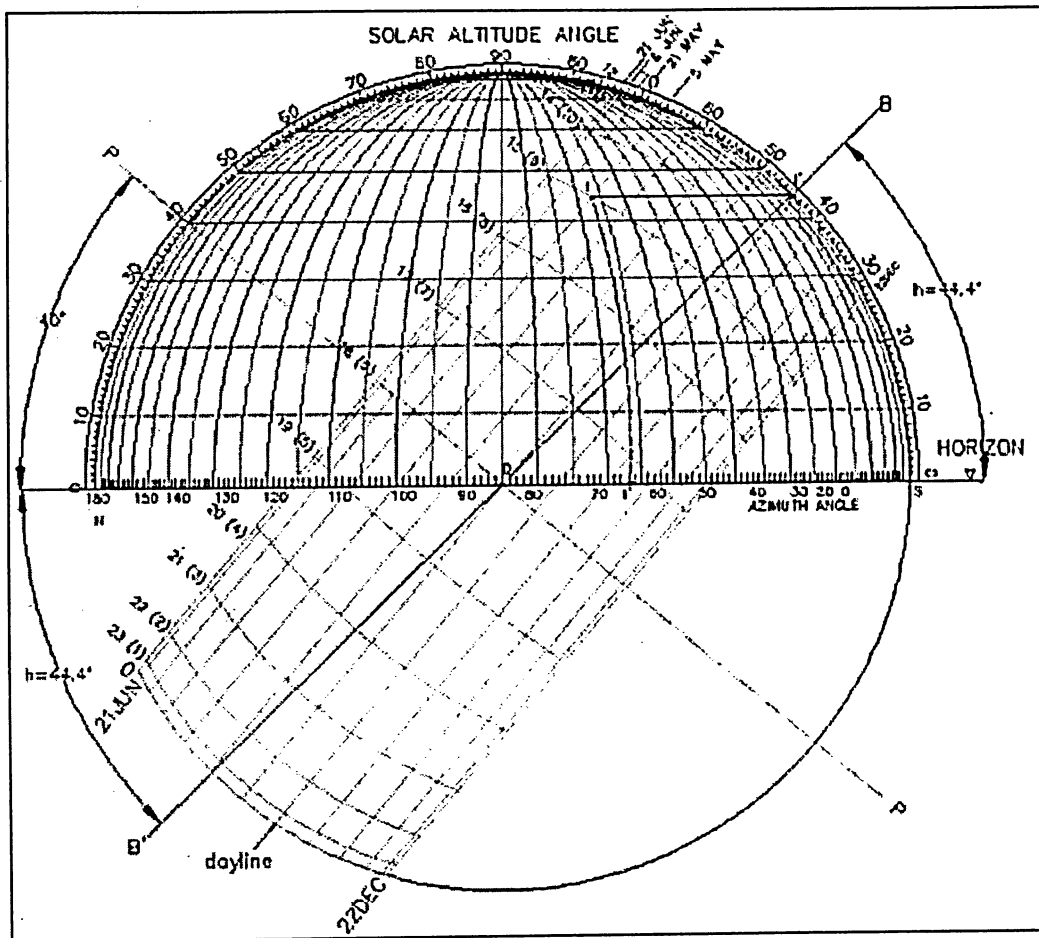
Although a PV-system installation based on solar module mounting angles of 30 and 60 degrees would improve the photovoltaic system's power output, the other mounting angles should not be ignored. For example, when trying to install a PV-system for a building located in downtown Toronto, shading produced by surrounding high-rises might pose an undesired limitation on the PV system installation. In this case, the PV module mounting angle of 0 deg should be investigated further in order to optimize the PV system performance. For a new building under construction, a PV module mounting angle of 90 deg should be considered. In new building constructions the solar modules

should be integrated into the building envelope in order to drive the construction materials cost down.

When testing the performance of photovoltaic arrays, the largest source of error in power ratings is often associated with the instrument and procedure used to quantify the solar irradiance. The difficulty arises from four sources that produce systematic influences on test results: photovoltaic modules respond to only a portion of the solar spectrum[16], devices used to measure solar irradiance may respond to all solar wavelengths or to a range similar to the photovoltaic modules, the optical acceptance angle or view angle of the module may differ significantly from that of the solar irradiance sensor, and the response of both the module and the solar irradiance sensor may vary significantly as a function of the solar angle-of-incidence. The concept of 'effective solar irradiance' provides a method for addressing the systematic influences and reducing the difficulty and uncertainty associated with field testing of arrays.

The incorporation of energy management techniques such as day light savings and smart sensors can significantly increase the reliability of the PV system. Building load can be significantly reduced by replacing incandescent loads with florescent loads. Florescent loads consume less energy while maintaining a satisfactory performance. Energy friendly building envelope can significantly reduce the electrical demand by heating loads and as a result reducing the load on the PV system.

Appendix A



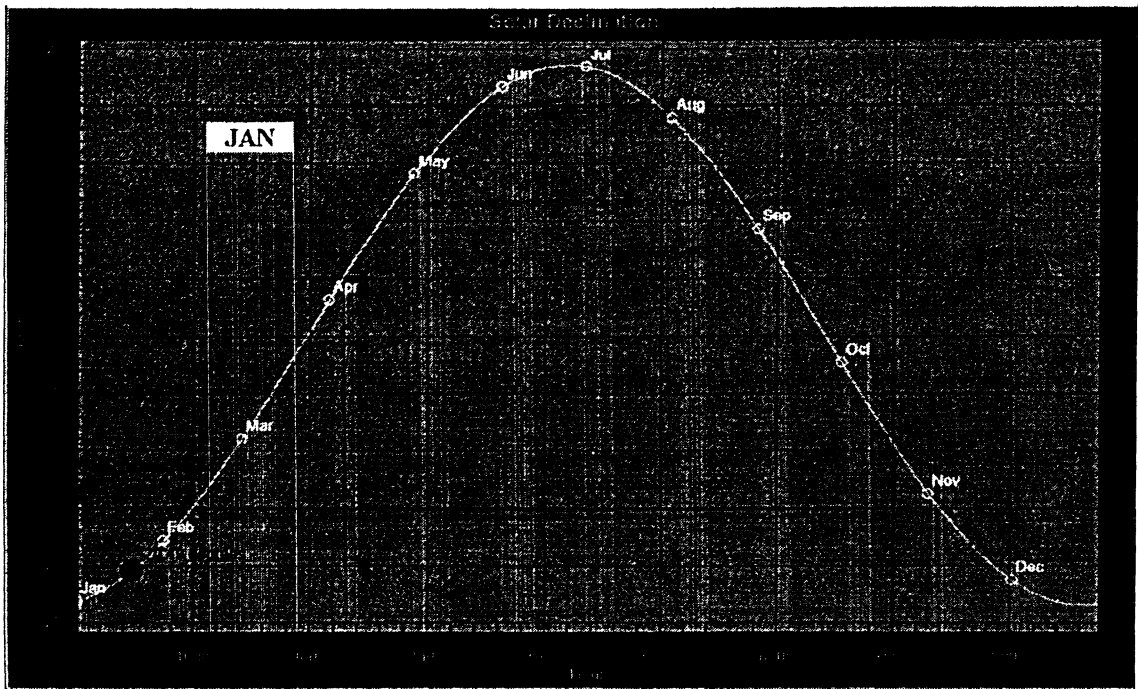
Listing of Computer Software

AutoCAD

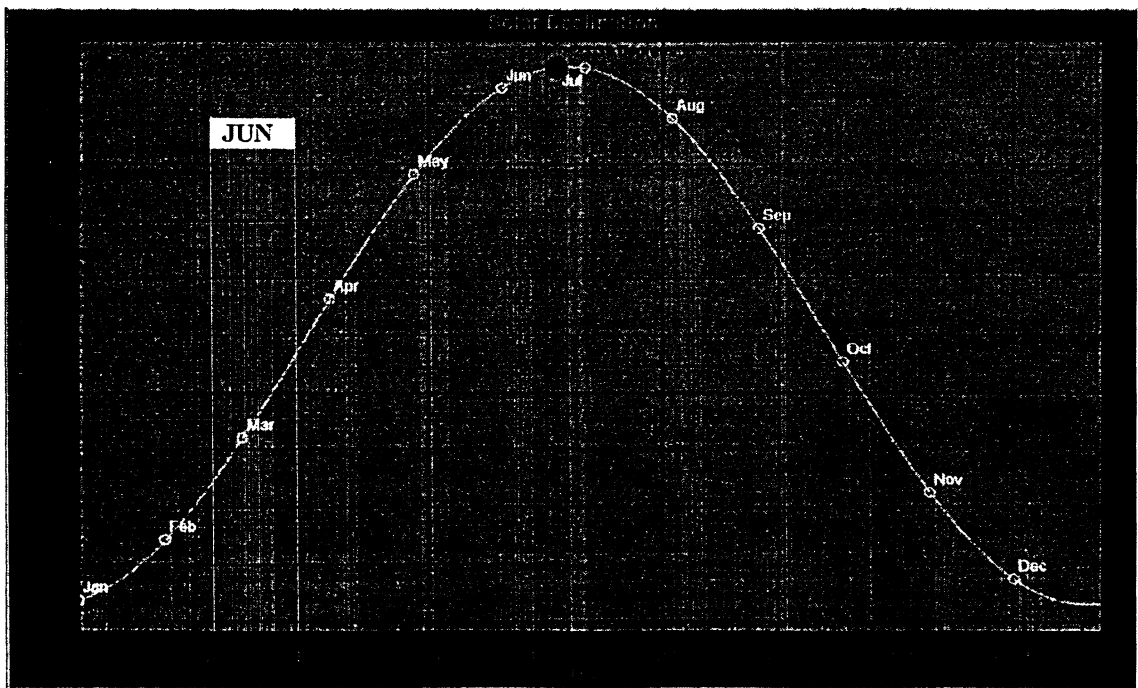
Microsoft Word

PV-DesignPro

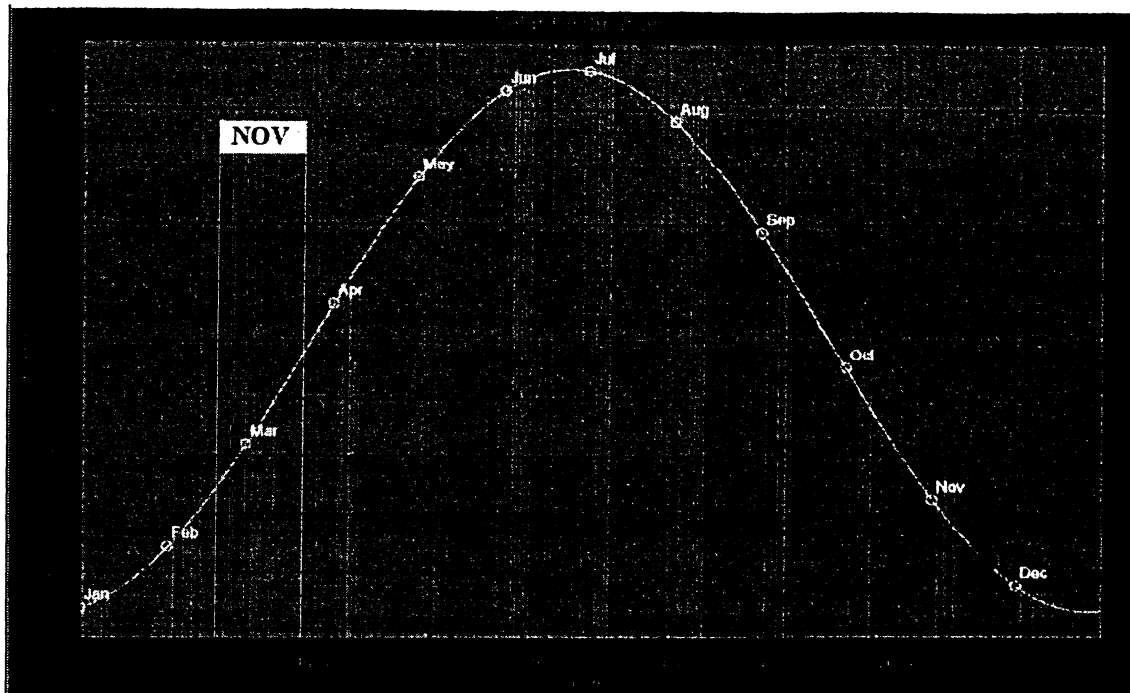
Appendix B



(A) Solar declination for the month of January



(B) Solar declination for the month of June



(C) Solar declination for the month of November

Bibliography

- [1] H.S. Rauschenbach. “*Solar Cell Array Design Handbook*” 1980. Van Nostrand Reinhold Company. NY.
- [2] GOLDENBERG, J., JOHANSSON, T.B., REDDY, A.K.N. & WILLIAMS, R.H., *Energy for a sustainable world*, John Wiley, New York, 1988.
- [3] HOHMEYER, O., *Social Costs of Energy Consumption*, Springer-Verlag, Berlin, 1988.
- [4] Natural Resources Canada. *Renewable Energy: The Future is Free*. 05/9/15
<http://oee.nrcan.gc.ca/Publications/infosource/Pub/ici/eii/M27-01-1472E.cfm>
- [5] Solar Buzz. *Solar Energy Costs/Prices*. 2007
http://searchnetworking.techtarget.com/sDefinition/0,,sid7_gci214351,00.html
- [6] Photovoltaic Systems Research & Development. *Design and Installation of PV Systems*. <http://www.linxtechnologies.com/docs/f_modules.html>
- [7] IEEE Std 739-1984, IEEE Recommended Practice for Energy Conservation and Cost Effective Planning in Industrial Facilities (ANSI).
- [8] D. King, W. Boyson, and J. Kratochvil, “Analysis of Factors Influencing the Annual Energy Production of Photovoltaic Systems,” *29th IEEE PV Specialists Conference*, 2002.
- [9] D. King, J. Kratochvil, and W. Boyson, “Measuring Solar Spectral and Angle-of-Incidence Effects on PV Modules and Solar Irradiance Sensors,” *26th IEEE PV Specialists Conference*, 1997, pp. 1113-1116.
- [10] D. King, J. Kratochvil, and W. Boyson, “Temperature Coefficients for PV Modules and Arrays: Measurement Methods, Difficulties, and Results,” *26th IEEE PV Specialists Conference*, 1997, pp. 1183-1186.
- [11] D. King and P. Eckert, “Characterizing (Rating) Performance of Large PV Arrays for All Operating Conditions,” *25th IEEE PV Specialists Conference*, 1996, pp. 1385-1388.
- [12] D. King, J. Kratochvil, and W. Boyson, “Field Experience with a New Performance Characterization Procedure for Photovoltaic Arrays,” *2nd World Conference on PV Solar Energy Conversion*, Vienna, 1998, pp. 1947-1952.
- [13] C. Whitaker, T. Townsend, J. Newmiller, D. King, W. Boyson, J. Kratochvil, D. Collier, and D. Osborn, “Application and Validation of a New PV Performance Characterization Method,” *26th IEEE PV Specialists Conference*, 1997, pp. 1253-1256.

- [14] B. Kroposki, W. Marion, D. King, W. Boyson, and J. Kratochvil, "Comparison of Module Performance Characterization Methods," *28th IEEE PV Specialists Conference*, 2000, pp. 1407-1411.
- [15] A. H. Fannery, et al., "Short-Term Characterization of Building Integrated Photovoltaic Modules", *Proceedings of Solar Forum 2002*, Reno, NV, June 15-19, 2002.
- [16] B. Kroposki, W. Marion, D. King, W. Boyson, and J. Kratochvil, "Photovoltaic Array Performance Model," Sandia National Laboratories , 2003.

Glossary

- IRRADIANCE:** is the amount of solar power impinging on a specific area, usually measured in units of W/m^2
- INSOLATION:** is the amount of solar energy received by a given area, measured in Wh/m^2
- PANEL:** a collection of modules mechanically fastened together, wired, and designed to provide a field-installable unit.
- PV ARRAY:** a mechanically integrated assembly of modules or panels with a support structure and other components, as required, including tracking apparatus where used, forming a power-producing unit.
- PV CELL:** the basic PV device that generates electricity when exposed to solar radiation.
- PV MODULE:** the smallest complete, environmentally protected assembly of PV cells, and other components normally sold by a manufacturer; comprised of several PV cells.
- PV SYSTEM:** all the components and subsystems that, in combination, convert solar energy into electrical energy suitable for connection to a load.
- STAND ALONE SYSTEM:** a PV system that supplies electrical energy without interconnection to any other power source.
- DECLINATION:** Solar declination is computed by hour in SunPlot3D. The angular position of the sun at solar noon with respect to the plane of the equator, north positive; $-23.45 \leq \text{declination} \leq +23.45$.
- ZENITH ANGLE:** The angle between the vertical and the line to the sun.
- SOLAR ALTITUDE:** The angle between the horizontal and the line to the sun.
- SOLAR AZIMUTH:** The angular displacement from south of the projection of beam radiation on the horizontal plane; east of south negative, west of south positive ($-90=E, +90=W, S=0, N=\pm 180$).
- MODULE SLOPE:** The angle between the plane of the surface and the horizontal; $0 \leq \text{slope} \leq +180$ (slope $> +90$ means the surface has a downward facing component).
- MODULE AZIMUTH:** The deviation of the projection on a horizontal plane of the normal to the surface from the local meridian, with zero due south, east negative, and west positive; $-180 \leq \text{azimuth} \leq +180$.
- ANGLE OF INCIDENCE:** The angle between the beam radiation on the module surface and normal to that surface.
- RATIO OF BEAM RAD. (R_b):** The ratio of beam radiation on the tilted module surface to that on a horizontal surface.
- TOTAL HORIZONTAL IRRADIATION (W/m^2) (H-Irr):** The sum of beam and diffuse radiation on a horizontal surface.
- MODULE IRRADIATION (W/m^2) (M-Irr):** Solar radiation on the tilted panel surface calculated using the Perez model.

Index

Abstract,iii
Acknowledgments, iv
Appendix A, 28
Appendix B, 29
Azimuth, 26, 30
Background, 1
Bibliography, 31
Cell PV, 32
Curve,power, 7
CirCAD, 28
Components List,42
Computer Software
 CirCAD, 28
 Microsoft Word, 28
Conclusions, 26
Design
 Flow Chart, 13
 Engineering, 14
DesignPro, iii,1,3,28
Declaration, ii
Declination, 29.30,32
Discussion, 20
Electrical/Computer Engineering
 Project, 2
Energy Conservation Opportunity, 24
Energy Management, 22
General Approach to the Problem, 3
Glossary, 32
Horizontal Irradiation, 32
Introduction, 1
Irradiance, 16, 32
Insolation,32
List of Figures, vii
List of Tables, vi
Literature Review, 6
Microsoft Word, 28
Module Irradiation (M-Irr), 16,21, 22, 32
Objectives, 1
Panel, 32
PV
 Array, 4, 32
 Cell, 32
 Module, 32
 System, 32
PV Design Pro, iii, 1, 3, 28
Recommendations, 26
Reversible, 9
Ratio of beam (Rb), 16, 21,22, 23, 32
Solution Methology, 11
Solar
 Altitude, 32
 Azimuth, 32
Stand Alone System, 32
Sun Plot 3D, 14 20
Simulation Results, 16
Statement of Problem, 11
Statement of Problem and Methodology
 of Solution, 11
Table of Contents, v
Vitae, 34

Vitae

NAME: Husam Alkhatib
PLACE OF BIRTH: KSA
YEAR OF BIRTH: 1980
BACHEOLER: University of Western Ontario
(1999-2003)
HONOURS and AWARDS: Recipient of the Millennium Scholarship